T.R.
GEBZE TECHNICAL UNIVERSITY
GRADUATE SCHOOL OF NATURAL AND APPLIED SCIENCES

DESIGN AND OPTIMIZATION OF A CAR SPRING UNDER AXIAL AND LATERAL LOADING

DUYGU BAŞARAN

A THESIS SUBMITTED FOR THE DEGREE OF
MASTER OF SCIENCE
DEPARTMENT OF MECHANICAL ENGINEERING

GEBZE
2019

T.R.

GEBZE TECHNICAL UNIVERSITY

GRADUATE SCHOOL OF NATURAL AND APPLIED SCIENCES

DESIGN AND OPTIMIZATION OF A CAR SPRING UNDER AXIAL AND LATERAL LOADING

DUYGU BAŞARAN

A THESIS SUBMITTED FOR THE DEGREE OF MASTER OF SCIENCE

DEPARTMENT OF MECHANICAL ENGINEERING

THESIS SUPERVISOR

ASSOC. PROF. DR. AHMET ZAFER ŞENALP

GEBZE

2019

T.C.
GEBZE TEKNİK ÜNİVERSİTESİ
FEN BİLİMLERİ ENSTİTÜSÜ

ARABA YAYININ EKSENEL VE YANAL YÜKLEME ALTINDA DİZAYNI VE OPTİMİZASYONU

DUYGU BAŞARAN
YÜKSEK LİSANS TEZİ
MAKİNA MÜHENDİSLİĞİ ANABİLİM DALI

DANIŞMANI
DOÇ. DR. AHMET ZAFER ŞENALP

GEBZE
2019

GEBZE TEKNİK ÜNİVERSİTESİ	**YÜKSEK LİSANS JÜRİ ONAY FORMU**

GTÜ Fen Bilimleri Enstitüsü Yönetim Kurulu'nun 03../.07.../..2019 tarih ve ..2019/...30.... sayılı kararıyla oluşturulan jüri tarafından 22/07/2019 tarihinde tez savunma sınavı yapılan Duygu BAŞARAN'ın tez çalışması Makine Mühendisliği Anabilim Dalında YÜKSEK LİSANS tezi olarak kabul edilmiştir.

JÜRİ

ÜYE
(TEZ DANIŞMANI) : Doç. Dr. AHMET ZAFER ŞENALP

ÜYE :Prof. Dr. MEHMET ALI ARSLAN

ÜYE : Yard. Doç. RAMAZAN ÜNAL

ONAY

Gebze Teknik Üniversitesi Fen Bilimleri Enstitüsü Yönetim Kurulu'nun

...../...../..... tarih ve ...../..... sayılı kararı.

SUMMARY

Suspension systems are one of the most important and essential equipment of land vehicles. Their main functions are road handling, steerability and driving comfort. Suspension system is composed of many equipments. In this thesis, helical springs are studied. For three different conditions (design, rebound and jounce), displacement are applied at the test machine to the springs, that are exposed to large deformation under the working conditions and reaction forces are achieved. Four spring models are chosen and analysed by finite element method and the result are compared to the test results. The analysis that resulted in the closest value to the test result is chosen as appropriate analyse type. Three of four springs that are chosen, have vertical and coincident spring and force axes. The other spring's force and spring axis is not vertical and coincident. Because of that skew axis, reaction force is composed of vertical and lateral forces when vertical force is applied to the spring. Optimization is conducted for lateral loaded spring. Six identical springs', which have the same coil path but different and varied wire diameter, CAD models are created in Creo Parametric and analysed by Ansys LS-DYNA. After the analyses, the optimum spring model is chosen.

Key Words: Car suspension springs, Finite element method, Lateral loaded spring, Reaction force, Axial load.

ÖZET

Süspansiyon sistemi kara araçlarının en önemli ve vazgeçilmez alt sistemlerinden biridir. Temel fonksiyonları; yol tutuşu, direksiyon hakimiyeti ve sürüş konforudur. Süspansiyon sistemleri birçok bileşenden oluşur. Bu çalışmada, helisel süspansiyon yayları incelenmiştir. Çalışma koşulları sırasında yüksek deformasyona uğrayan bu yaylara dizayn, sıkıştırma ve serbest hal olmak üzere 3 durum için yer değiştirme değerleri test makinesinde uygulanmış ve tepki kuvvetleri ölçülmüştür. Seçilmiş olan 4 adet yay bazı sonlu elemanlar yöntemleriyle analiz edilip, çıkan sonuçlar test sonuçları ile karşılaştırılmıştır. Test sonucuna en yakın değeri veren analiz yöntemi, en uygun sonlu elemanlar yöntemi seçilmiştir. Seçilmiş olan 4 adet yayın 3' ünün kuvvet ve yay ekseni çakışık ve diktir. Diğer yayın ise kuvvet ve yay ekseni eğridir ve çakışık değildir. Eğri eksen sebebiyle, uygulanan dik kuvvete karşı oluşan tepki kuvveti hem dik hem de yanal bileşene sahiptir. Yanal yüklü bu yay için optimizasyon yapılmıştır. İlgili yaya özdeş (aynı sarım yoluna sahip) 6 değişken kesit çapına sahip yay, Creo Parametric çizim programıyla modellendi ve Ansys LS-DYNA ile analizi yapıldı. Analizler sonucunda en uygun yay çapına karar verildi.

Anahtar Kelimeler: Otomobil süspansiyon yayları, Sonlu elemanlar yöntemi, Yanal yüklü yay, Tepki kuvveti, Eksenel yük.

ACKNOWLEDGEMENTS

I would like to express my deep and sincere gratitude to my supervisor, Assoc. Prof. Dr. Ahmet Zafer Şenalp, who not only shared his profound scientific knowledge with me but also thaught me great lessons of life. Also, I would like to thank Rözmaş company. Their support, suggestions and encouragement gave me the drive and will to complete this work.

I am grateful to my parents for their love and support.

TABLE of CONTENTS

	Page
SUMMARY	v
ÖZET	vi
ACKNOWLEDMENTS	vii
TABLE of CONTENTS	viii
LIST of ABBREVIATIONS and ACRONYMS	x
LIST of FIGURES	xi
LIST of TABLES	xv
1. INTRODUCTION	1
1.1. Purpose and Scope of Thesis	1
2. SUSPENSION SYSTEM	6
2.1. Suspension System Types	6
2.1.1. Dependent Suspension System	6
2.1.2. Independent Suspension System	8
2.1.2.1. Double Wishbone Suspension System	10
2.1.2.2. Multi-Link Suspension System	11
2.1.2.3. MacPherson Strut Suspension System	13
2.2. Suspension System Basic Parts	15
2.2.1. Shock Absorber	15
2.2.2. Anti-Sway Bar	17
2.2.3. Springs	18
2.2.3.1. Coil Springs	19
2.2.3.2. Leaf Spring	20
2.2.3.3. Torsion Bar	21
2.2.3.4. Pigtail Spring	23
3. SPRINGS USED IN THE STUDY	25
3.1. Spring Models	25
3.1.1. 2319 Model Spring	25
3.1.2. 2299A Model Spring	26
3.1.3. 2309 Model Spring	27

3.1.4. 2304A Model Spring 28
4. ANALYSIS OF SPRINGS 31
4.1. Analyse Types Used for Spring Models 31
4.1.1. Static Structural Analyse 31
4.1.2. Transient Structural Analyse 35
4.1.3. Workbench LS-DYNA 36
4.2. Analysis of Spring Models 39
4.2.1. Analyse of 2319 Model Spring 43
4.2.2. Analyse of 2299A Model Spring 50
4.2.3. Analyse of 2309 Model Spring 60
4.2.4. Analyse of 2304A Model Spring 69
4.3. Analysis of Spring Models by LS-DYNA 72
4.4. Optimization of 2304A Spring Model 74
5. CONCLUSION 76

REFERENCES 77
BIOGRAPHY 79

LIST of ABBREVIATIONS and ACRONYMS

Abbreviations and Acronyms		**Explanations**
c	:	Damping Coefficient
u	:	Displacement
ύ	:	Velocity
ü	:	Acceleration
m	:	Mass
k	:	Stiffness
o.d.e	:	Ordinary differential equation
ω	:	Angular velocity
T	:	Period
$u0$	:	Initial displacement
ύ0	:	Initial velocity
3D	:	Three dimension
C	:	Carbon
Si	:	Silicon
Mn	:	Manganese
P	:	Phosphorus
S	:	Sulfur
Cr	:	Chromium
N	:	Newton
Mpa	:	Mega Pascal
mm	:	Milimeter
CAD	:	Computer Aided Design
dof	:	Degree of freedom
FEM	:	Finite Element Method
FEA	:	Finite Element Analysis

LIST of FIGURES

Figure No:		Page
2.1:	Mutual ifluence of the two wheels of a rigid axle.	7
2.2:	Beam axle amd leaf spring.	7
2.3:	Twist axle with trailing arm.	8
2.4:	The independent suspension system.	9
2.5:	Double wishbone suspension system.	11
2.6:	Multi-Link suspension system.	12
2.7:	MacPherson strut suspension system.	14
2.8:	Shock absorber.	16
2.9:	Anti-Sway bar.	17
2.10:	Coil springs.	20
2.11:	Leaf springs.	21
2.12:	Torsion bar.	22
2.13:	Double pigtail spring.	24
2.14:	Single pigtail spring.	24
3.1:	2319 model spring 3D geometry.	25
3.2:	2299A model spring 3D geometry.	26
3.3:	2309 model spring 3D geometry.	27
3.4:	2304A model spring 3D geometry.	27
3.5:	Lower plate of 2304A model spring.	28
3.6:	Geometry of 2304A model spring	29
4.1:	Position vectors and motion of a deforming body.	32
4.2:	Polar decomposition of a shearing deformation.	34
4.3:	Single degree of freedom damped system.	36
4.4:	Forces acting on mass, m.	36
4.5:	Stress - strain graph of 54SiCr6.	39
4.6:	Contact region of springs.	41
4.7:	Target and contact region between spring and plate.	41
4.8:	Details of Body Interaction in LS-DYNA.	42
4.9:	Mesh view of 2319 model spring.	43

4.10:	Total deformation of 2319 model spring under 126,22 mm displacement, Ansys (Static & Transient) analysis.	46
4.11:	Total deformation of 2319 model spring under 126,22 mm displacement, LS-DYNA analysis.	46
4.12:	Total deformation of 2319 model spring under 160,22 mm displacement, Ansys (Static & Transient) analysis.	47
4.13:	Total deformation of 2319 model spring under 160,22 mm displacement, LS-DYNA analysis.	48
4.14:	Total deformation of 2319 model spring under 176,22 mm displacement, Ansys (Static & Transient) analysis.	49
4.15:	Total deformation of 2319 model spring under 176,22 mm displacement, LS-DYNA analysis.	49
4.16:	Mesh view of 2299A model spring.	50
4.17:	Total deformation of 2299A model spring under 76,7 mm displacement, Ansys (Static Large Def. Off) analysis.	53
4.18:	Total deformation of 2299A model spring under 76,7 mm displacement, LS-DYNA analysis.	53
4.19:	Total deformation of 2299A model spring under 76,7 mm displacement, Ansys (Transient Structural) analysis.	54
4.20:	Total deformation of 2299A model spring under 76,7 mm displacement, LS-DYNA analysis.	54
4.21:	Total deformation of 2299A model spring under 101,7 mm displacement, Ansys (Static Large Def. Off) analysis.	55
4.22:	Total deformation of 2299A model spring under 101,7 mm displacement, Ansys (Static Large Def. On) analysis.	56
4.23:	Total deformation of 2299A model spring under 101,7 mm displacement, Ansys (Transient Structural) analysis.	56
4.24:	Total deformation of 2299A model spring under 101,7 mm displacement, LS-DYNA analysis.	57
4.25:	Total deformation of 2299A model spring under 126,7 mm displacement, Ansys (Static Large Def. Off) analysis.	58

4.26:	Total deformation of 2299A model spring under 126,7 mm displacement, Ansys (Static Large Def. On) analysis.	58
4.27:	Total deformation of 2299A model spring under 126,7 mm displacement, Ansys (Transient Structural) analysis.	59
4.28:	Total deformation of 2299A model spring under 126,7 mm displacement, LS-DYNA analysis.	59
4.29:	Mesh view of 2309 model spring.	60
4.30:	Total deformation of 2309 model spring under 71,06 mm displacement, Ansys (Static Large Def. Off & On, Transient) analysis.	63
4.31:	Total deformation of 2309 model spring under 71,06 mm displacement, LS-DYNA analysis.	63
4.32:	Total deformation of 2309 model spring under 144,06 mm displacement, Ansys (Static Large Def. Off) analysis.	64
4.33:	Total deformation of 2309 model spring under 144,06 mm displacement, Ansys (Static Large Def. On) analysis.	65
4.34:	Total deformation of 2309 model spring under 144,06 mm displacement, Ansys (Transient Structural) analysis.	65
4.35:	Total deformation of 2309 model spring under 144,06 mm displacement, LS-DYNA analysis.	66
4.36:	Total deformation of 2309 model spring under 174,06 mm displacement, Ansys (Static Large Def. Off) analysis.	67
4.37:	Total deformation of 2309 model spring under 174,06 mm displacement, Ansys (Static Large Def. On) analysis.	67
4.38:	Total deformation of 2309 model spring under 174,06 mm displacement, Ansys (Transient Structural) analysis.	68
4.39:	Total deformation of 2309 model spring under 174,06 mm displacement, LS-DYNA analysis.	68
4.40:	Mesh view of 2304A model spring.	69
4.41:	Mesh of 2304A model spring parts.	70
4.42:	Analysis settings of 2304A model spring.	71
4.43:	Total deformation of 2304A model spring under 181 mm displacement, LS-DYNA analysis.	72

4.44: Analysis Settings in LS-DYNA analyse. 73
4.45: 2304A spring model top & bottom wire diameter. 75
5.1: Self contact condition 77

LIST of TABLES

Table No:		Page
3.1:	Properties of 2319 model spring.	25
3.2:	Properties of 2299A model spring.	26
3.3:	Properties of 2309 model spring.	27
3.4:	Force center point of ends of 2304A model spring.	29
3.5:	Properties of 2304A model spring.	29
4.1:	The chemical composition of the material.	38
4.2:	The properties of the spring material.	38
4.3:	Plastic stress-strain values of the spring material.	40
4.4:	The properties of the plate material	40
4.5:	The element size, element number and node number of 2319 model spring	43
4.6:	Boundary conditions for static structual analyse of 2319 model spring.	44
4.7:	Boundary conditions for transient structual analyse of 2319 model spring.	44
4.8:	Boundary conditions for LS-DYNA (Explicit) analyse of 2319 model spring	45
4.9:	Comparison of calculated reaction forces for applied displacement 126,22 mm	45
4.10:	Comparison of calculated reaction forces for applied displacement 160,22 mm	46
4.11:	Comparison of calculated reaction forces for applied displacement 176,22 mm.	46
4.12:	The element size, element number and node number of 2299A model spring	47
4.13:	Boundary conditions for static structual analyse of 2299A model spring.	48
4.14:	Boundary conditions for transient structual analyse of 2299A model spring.	48
4.15:	Boundary conditions for LS-DYNA (Explicit) analyse of 2299A model spring.	49

4.16: Comparison of calculated reaction forces for applied displacement 76,7 mm. 49
4.17: Comparison of calculated reaction forces for applied displacement 101,7 mm. 50
4.18: Comparison of calculated reaction forces for applied displacement 126,7 mm. 50
4.19: The element size, element number and node number of 2309 model spring. 51
4.20: Boundary conditions for static structual analyse of 2309 model spring. 52
4.21: Boundary conditions for transient structual analyse of 2309 model spring. 52
4.22: Boundary conditions for LS-DYNA (Explicit) analyse of 2309 model spring. 53
4.23: Comparison of calculated reaction forces for applied displacement 71,06 mm. 53
4.24: Comparison of calculated reaction forces for applied displacement 144,06 mm. 54
4.25: Comparison of calculated reaction forces for applied displacement 174,06 mm. 54
4.26: The element size, element number and node number of 2304A model spring. 55
4.27: Boundary conditions for LS-DYNA (Explicit) analyse of 2304A model spring. 56
4.28: Comparison of calculated reaction forces for applied displacement 181 mm. 57
4.29: Boundary conditions for each spring model. 59
4.30: Results for each spring model. 59
4.31: Results for different wire diameter. 60

1. INTRODUCTION

Suspension system is used in vehicles to reduce road effects and vibration. Passengers feel a lot of vibration when a car runs because of rough roads and car engine vibration. If a car was rigid, this vibration would be transmitted into whole body of the car which could damage the vehicle and makes the journey uncomfortable for the driver. Suspension system does not only smooth out the drive but also keeps the vehicle in control. It maximizes the friction between the wheels and the road so steering stability and road holding can be achieved. Designing the suspension system is not easy so it has been a challenging topic for the engineers for a long time. For a good design, engineers should determine the objectives well and choose the proper parameters that influence the objectives most. Some duties of a suspension system are;

- Sustain correct car ride height
- Isolate the vehicle from the road's disturbing effects
- Decrease shock forces of the road
- Sustain wheel aligment
- Balance the static weight of the vehicle
- Keep the wheels in contact with the road
- Reduce the engine vibration
- Control the vehicle's way of ride

1.1. Purpose and Scope of Thesis

It is widely known that suspension system is an important component for a vehicle. It is mentioned before that roads are not perfectly flat and smooth. Also, when the car engine runs, it vibrates and make the passengers feel uncomfartable. that the surface is not perfectly flat or smooth. Suspension system aims to minimise the effect of road irregularities and engine vibration. There are some suspension system kinds and it is up to vehicle's tpye and road which vehicle will take. Additionally, suspension system components depend on the type of suspension system. Another important issue is production of the suspension system. As it is known, car industry is competitive. So

companies should be fast as much as they could. Some companies obtains the spring's dimesions and shapes according to theoretical and ampirical calculations. After production, they have to test to be sure before the assembly to the car. Some springs satisfy the expected forces but others fail and which leads to waste of money and time.

There are certain publications about the helical springs that are helpful to this work. Some researchers, have contributed to this topic, and their works are reviewed in this section.

In 2008, Prawoto, Ikeda, Manville and Nishikawa searched about automotive suspension coil springs, its materials characteristic, their fundemental stress distribution, its manufacturing and common failures. They went on detail discussed about the parameters which influence the quality of coil springs in detail. The paper reviewed may case studies of suspension spring failures. The failures have a wide range. They started from the very basic that include insufficient load carrying capacity and continued with raw material defects, for instance excessive inclusion levels. The other failure were manufacturing defects such as delayed quench cracking, failures due to complex stress usage and chemically induced failure. Finite element analysis is applied to find the stress distributions around typical failure initiation sites [10].

In 2017, Thakare and Kadlag worked on premature failure of helical compression spring and tried to improve the service life of it. They tried to find the optimum design. To achieve it, spring models which have different wire diameter, are analysed and results show that the stresses are decreased with increased wire diameter and number of turns of coil spring. Existing and new spring are determined and mathematical analysis carried out on them. Both of them have different characteristics and material ingredient. Multi objective optimization on the basis of ratio analysis (MOORA) method is used for material selection criteria for a new spring. Moreover, stress and deformation analysis are conducted by ANSYS software. The new spring is tested by load testing machine and results of experiment and ANSYS are compared. Both results have shown that the deflection in the spring decreases with reduction in the stresses when change in certain parameters. Also, they have seen that the number of turns influences the deflection and stress inversely. This effect can exist if the wire diameter changes because wire diameter has the influence on the deflection and the stresses. Thereby, if the wire diameter increaes, the deflection and stresses also decreases [4].

In 2014, Youli, Yanli and Yuanlin tried to find out why a compression coil spring fractured at the transition position although the nominal stress here is less than the point that is at the inside of the fully active coil. They have utilized visual observations and seen that when a wear scar was formed on the first active coil, the fracture surface showed radiating ridges arising from the existing wear scar. Stress analysis are carried out and it is indicated that stress singularities existing are at the edges of the contact zone, where cycle slip and fatigue crack nucleation enable. Lastly, they extrapolated that fatigue crack initiation of the suspension spring exist at the contact position that have corrosion and stress singularities. When an initial crack was existed, it was forced to propagate along the direciton of 45° with the spring wire axis because the maximum principal tensile stress forces the crack to improve. They suggested to use solid lubrication film in the closed ends to reduce the corrosion and fretting [19].

In 2010, Pollanen and Martikka prepared a full 3D solid model and conducted FEM analysis with MSC Nastran to find stress, strain deformation, natural frequencies and modes. All these works were made to find an optimum design of the spring which aimed to minimize volume of wire due to space restriction, desired spring rate, avoidance of surging frequency and achieving reliably long fatigue life [9].

In 2013, Gundre and Wankhade conducted the finite element analysis of a helical spring. Elastic characteristics and the fatigue strength are important in the design of helical springs. These springs have to work under very high loadings so engineer should have been sure that they could afford the relative loadings. So for this purpose linear static analysis was conducted to determine the stress and strain results from the finite element model. The material used in this study is linear elastic and isotropic. The results have shown that classical spring model is not suitable when dealing with these spring geometries. Finally, the analysis shows that the shear stress has maximum value at the inner side [3].

In 2005, Berger and Kaiser investigated when very high cycle fatigue test is applied on helical compression springs, external compressive forces and torsional stresses exist on the relating helical spring. These investigations added a significant contribution to the experience of fatigue behaviour in the very high cycle regime [5].

In 2010, Kaou, Tabibi, Benghamen, Azouaoui and Azzaz studied the spring mechanical behaviour under tensile axial loading by preparing a 3D geometric model of a twin helical spring and conducting its finite element analysis. The model had18-dof and “wired-shape” of spring is used to discretise the complex model. Axial load

was applied and mechanical response of the twin spiralled helical spring was obtained. The analysis showed that both the evolution of the theoretical and the numerical tensile and compression normal stresses have sinusoidal behaviour. The overall equivalent stress isovalues increased radially from 0° to 180° and reached to the maximum value on the internal radial zone at the section 180°. However, the minimum stress level is located in the centre of the filament cross section [6].

In 2016, Sequira, Singh and Shetti compared the properties of composite and steel helical spring and the tried to decide the factors that influence the stiffness to weight ratio. Spring geometry is modeled in CREO software and analysed by FEM under different loading condition. The results of the analytical calculations and FEA results were compared and just 13% error is established. Also to decide the kind of the material for spring manufacturing, the specific modulus of steel (25,47), Kevlar (21,42) and carbon (43,75) are compared and it has concluded that carbon has high stiffness to weight ratio compared to the other materials, so to use carbon as material of spring instead of steel is useful to decrease the overall weight of the vehicle [12].

In 2014, Razooqi, Ameen and Mashloosh aimed to determine the stiffness of a circular cross-section helical coil compression spring and slotted cylinder springs which are subjected to axial loads under static and dynamic conditions. Five examples of the spring geometry are used. Both theoretical and finite element models are developed to calculate the spring stiffnesses. A FEM was generated via ANSYS software. Moreover, mode shapes, transient response of springs and the natural frequencies are obtained. In conclusion, the stiffness values were obtained by using the theoretical methods and obtained from the FEA compared and the results were close. Also, it has found that the stiffness of spring for slotted cylinder spring is much larger than that for helical spring. If the number of slots per section increase, the stiffness of slotted cylinder spring increases as well. Mode shape, transient response and natural frequencies of helical spring and slotted cylinder spring have been obtained and results have been compared. It has been found that the natural frequency is directly proportional to the stiffness [1].

Within this thesis, to reduce waste of money and time, Rozmas wants to use FEM and Ansys software. Because the firm is new at FEM, a correlation between test experiment results and Ansys result is needed. Test results and Ansys results are compared. Some Ansys analyse module has been tried (static structural, transient structural and LS-DYNA) and the best method has been found. In the second chapter

the vehicle suspension system and their components are explained. In the third chapter, spring models and their properties are explained. In the fourth chapter, what kind of analysis types are applied is explained. Also, their theory and solution method is explained. The spring models are analysed by different methods and their results are compared with test results. In the fifth and last chapter, some inferences are deduced according to numerical results that are got in the previous chapter.

2. SUSPENSION SYSTEM

A suspension system's main purpose is to protect the vehicle from the external factors. By means of the purpose, the ride becomes safer and comfortable. Also suspension system improves the life of the vehicle. Aims of suspension system can be listed like below;

- Protects the vehicle from damage.
- Contributes to the car's handling and braking.
- Supports the weight.
- Keeps the wheels contact with the road.
- Keeps the wheels in correct aligment by working with the steering system.
- Provides a smooth ride.
- Lets front wheels to run side-to-side for steering.
- Protects passenger and cargo from vibration and shock
- Allows rapid cornering with a stability.

2.1. Suspension System Types

There are certain kinds of suspension system used in cars according to their requirements. Suspension systems are classified into 2 subgroups: dependent and independent suspension. Moreover, they are classified further into many types which are explained extensively in the following sections.

2.1.1. Dependent Suspension System

A dependent suspension system has a beam or live axle that holds wheels parellel to each other and perpendicular to the axle with the help of leaf springs to it [10]. When a force acts on a wheel because of road distortion, the other coupled wheel is affected as well. Also, if the camber of one wheels changes, the camber of the opposite wheel follows the same way. Dependent suspension system uses constant camber, it is usually used in vehicles that carry heavy loads [10]. Because it can absorb more shocks

than independent suspension system. Mutual influence of the two wheels of a rigid axle is shown in Figure 2.1 [24].

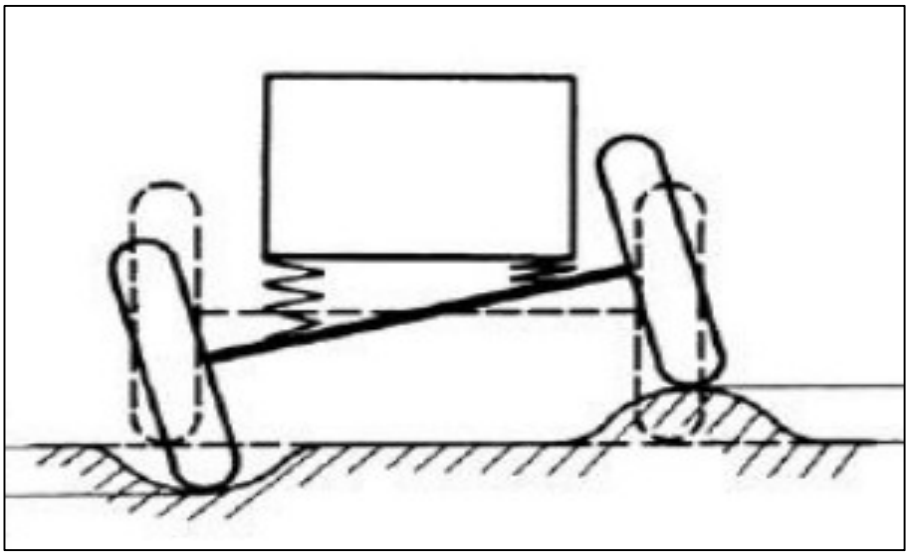

Figure 2.1: Mutual influence of the two wheels of a rigid axle.

Beam axle and leaf spring is shown as an example of dependent suspension system in Figure 2.2 [25].

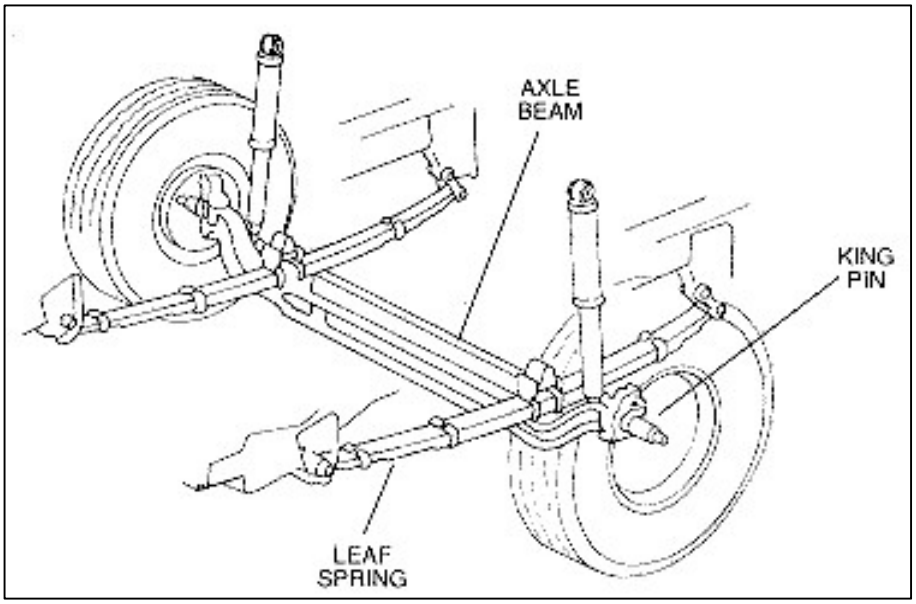

Figure 2.2: Beam axle and leaf spring.

Twist axle with trailing arm is shown together in Figure 2.3 [24].

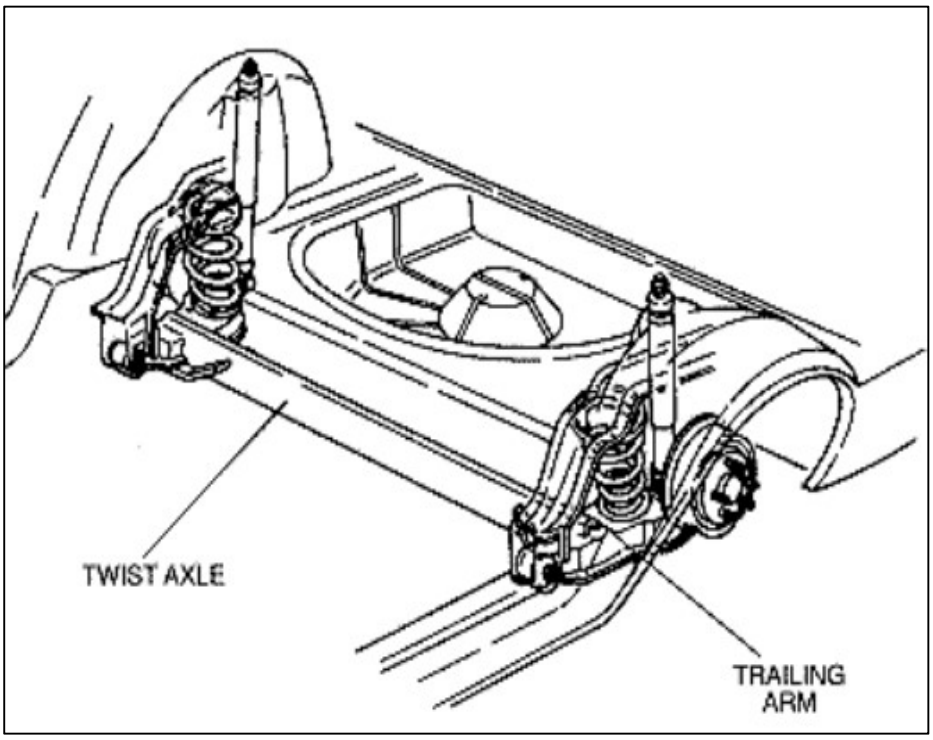

Figure 2.3: Twist axle with trailing arm.

2.1.2. Independent Suspension System

Wheels belong to an independent suspension system are allowed to move up and down on their own without effecting the opposite wheels by using kinematic linkages and coil springs. Suspensions with anti-roll bars that link the wheels are also mentioned as independent suspension system [14]. A car with independent suspension, is exposed to many different forces because each wheel is attached separately to the car body, so allowing it to move independently from each other.

The independent suspension system, has an important advantage. It requires less space than dependent suspension system and because of this advantage most of the passenger vehicles and light cars prefer independent suspension system. Also it has a better resistance in steering vibration because the independent suspension system connects the wheels to the frame.

Independent suspension system seems to be advantageous mentioned at previous paragraph but that is not the case. Disadvantages of independent suspension system can be listed like this,

- complicated design
- producing cost due to high number of parts
- requirements of more rigid chassis or sub-frame structure
- transmitting effects of unbalanced wheel assembly to the steering wheel more easily

In today and the past, designers and manufacturers of the vehicles are interested in the development process for suspension system. Design constraints, needs, conceptual design, suspension kinematics, behaviour of structure system, and etc. should be considered during development process, All these studies and efforts aims to obtain the optimal suspension geometry in order to equip a vehicle with right suspension system [15]. Independent suspension system requires more engineering effort and expense in development versus dependent suspenison system. Also independent suspension system is a complex suspension system and it can require higher manufacturing costs. However, it is prefered commonly because provides more comfortable drive than dependent suspension system. When one wheel push up, other wheel does not be effected as shown in Figure 2.4 [20].

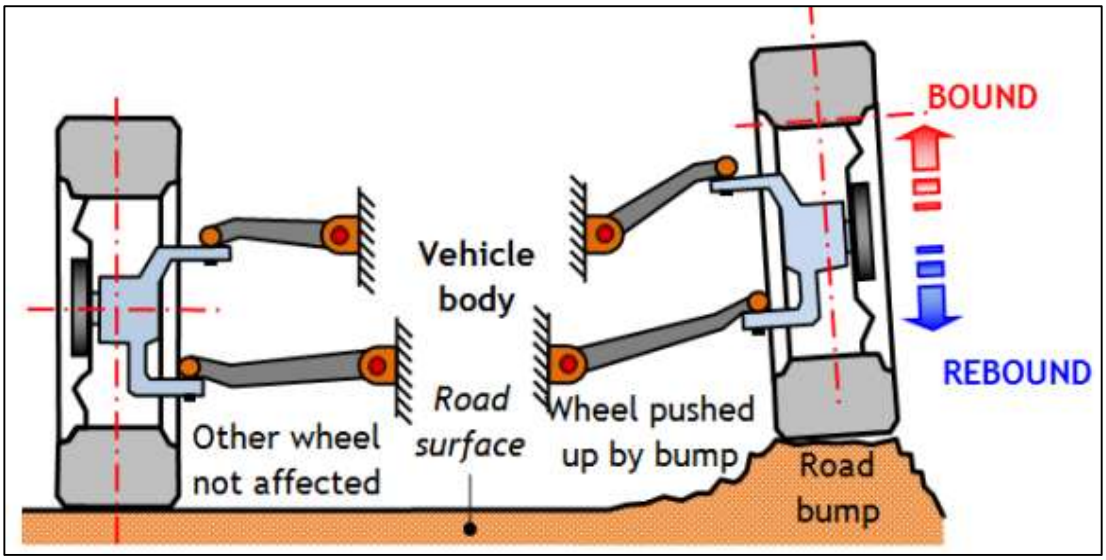

Figure 2.4: The independent suspension system.

Engineers have tried to develop independent suspension system for a long time and some speacial types has been developed, such as MacPherson, double wishbone, multi-link, trailing arm and swing axle. Some of these examples have been scrapped for different reasons, with only basic concepts, MacPherson strut, double wishbone and multi-link suspension system, have been used in high number of the vehicle.

2.1.2.1. Double Wishbone Suspension System

Double wishbone suspension system uses two "A" shape arms, one place on the top and the other in the bottom. It is commonly used for the suspension of small trucks and passenger cars. In this type of suspension, wheels are bonded to the vehicle body by upper and lower "A" shaped arms. Double wishbone suspension system allows you to design the geometry in regard to the length of the upper and lower arms and their bonding angles. There is one important point that should be taken care. The upper and lower arms should not have equal length because in this case the tread and the tire to ground camber of the tire will change. So it will make impossible to acquire enough cornering performance. Engineers solve this problem by designing the upper arm shorter than the lower arm so that the tread and the tire to ground camber of the tire fluctuate less. Making the lower arm shorter is widely used in many cars.

The double wishbone suspension system is a group of space RSSR (revolute joint-spherical joint-spherical joint-revolute joint) four-bar linkage mechanisms. Its kinematic relations are complex and performance is low. So, rational settings of the position parameters of the guiding mechanism are essential to ensure a good performance of the independent double wishbone suspension [17].

Double wishbone suspension system have some advantages. For instance, upper and lower suspension system allows the vertical suspension movement so the negative camber increases. Also, it is flexible to be design. The arms of the system can be adjusted with different angle to the surface. Additionally, some paramaters such as camber gain, swing arm length etc. can be determined according to the ride condition. Although double wishbone suspension system has some advantages, it is not always preferred because it has some disadvantages. For example, it is complicated to design and expensive for manufacturing. It has many components so if one component fail, it will effect whole system. Because of the large number of components, it is heavier

than an equivalent MacPherson design. As it is mentioned before, extra weight is not a preferred choice for the car design. Lastly, double wishbone suspension system is usually used at the rear end of the car and it is a limiting property for car manufacturers. Double wishbone suspension system can be understand from Figure 2.5 [20].

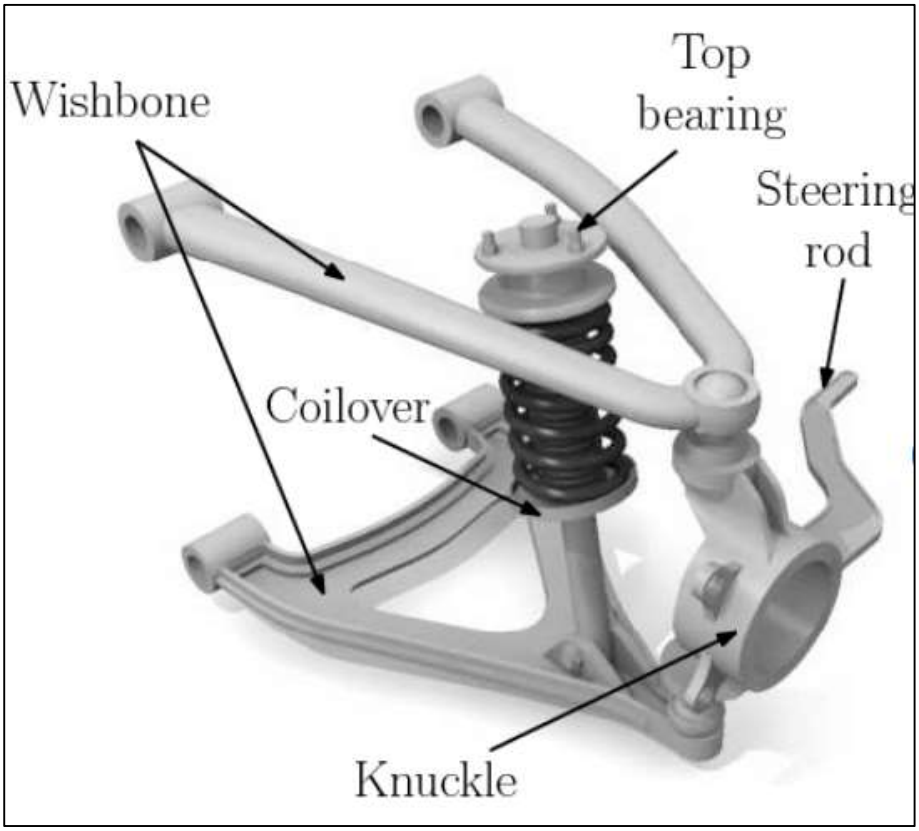

Figure 2.5: Double Wishbone suspension system.

2.1.2.2. Multi-Link Suspension System

Multi-link suspension system is another type of independent suspension system. the latest development in road car chassis design. It provides high stiffness in lateral direction and a reasonable compliance in the fore/aft direction. Its mechanism is useful for vehicle that travels rough roads such as terrain vehicles. It provides a good ride quality without affecting handling and safety. Multi-link suspension system is developed from the double wishbone susupension system. It has more links that are hinged about a point on the body or subframes using a bush or a ball joint and these links do not have to be of equal length. Due to this multiple links, a designer can change

a suspension parameter independently and it means, a designer have a good control over the ride.

Multi-link suspension system seems like a good because it has many advantages but this is not the case. Because it is a complex system to design and has high manufacture cost. It is preferred for luxury cars mostly. An example of Multi-Link suspension system is shown in Figure 2.6 [21].

Figure 2.6: Multi-Link suspension system.

2.1.2.3. MacPherson Strut Suspension System

Another type of independent suspension system is MacPherson strut suspension system. It is widely used today. This strut was designed by Earles S. MacPherson in 1949 for Ford Motor Company and named after the designer. A strut includes springs and shock absorbers.

The MacPherson can be used for both front and rear suspensions, but generally mounted at the front of the car. The MacPherson strut normally also has a steering arm built into the lower inner portion. This assembly is so simple that can be pre manufactured into a unit. By removing the upper control arm, it follows for more width in engine bay, aiding in many maintenance work or engine design requirements. MacPherson suspension system does not require a large space in the engine part. This system is used as the front suspension in the car and suspension system is generally used for better cornering and also for the comfortable passenger travel. MacPherson suspension system contains upper bonding point, shock absorber, spring leg and lower control arm. If the system contains only one lower arm, it is called as single wishbone system [13].

The main advantage of MacPherson struts is to be the most compact and have least weight as an independent suspension system. Second advantage is to be less expensive than other independent suspension systems becuse the upper control arm is entirely eliminated so it requires less components. The simplicity of MacPherson strut system provides an easier design than other independent suspension system and less cost. It is widely used in front of the car but some vehicles used it for all corners such as Lancia Delta.

Although MacPherson strut suspension is widely preferred, it has some disadvantages. The geometry of MacPherson strut allows the repairing easily but when the vertical position of the wheel changes, the camber angle necessarily changes and this is an unwanted situtation. When comparing to the other independent suspension systems, it is seen that MacPherson strut does not allow vertical movement of the wheel without some degree of either camber angle change, sideway movement or both. It means that it does not allow a good handling like double wishbone and multi-link suspension system. The direction of MacPherson strut is vertical so it tends to transmit vibration and roads irregularities directly to the car. It makes the ride uncomfartable

so manufacturers needs to add extra vibration reducing equipments. MacPherson strut suspension system and its parts is shown in Figure 2.7 [22].

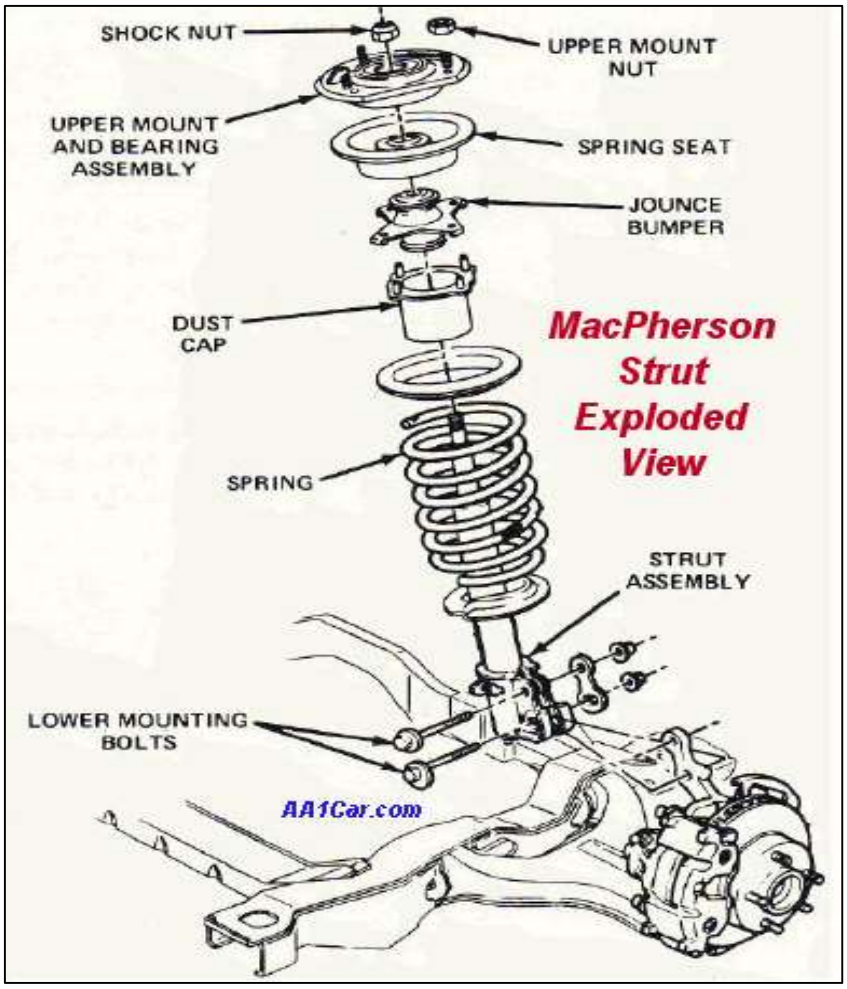

Figure 2.7: MacPherson strut suspension system.

2.2. Suspension System Basic Parts

A car's suspension system composed of individual suspension components, non-suspension system, hardware and design. All of them work together and ensure a safe and comfortable ride. If the system is examined in detail, it can be seen that there are dozens of different components, but here the main interest is focused in four basic parts of a car suspension system and they are shock absorber, anti-sway bar, and springs.

2.2.1. Shock Absorber

A shock absorber works with a spring and it slows down the springing action of the suspension springs. Also it is fiiled with hydraulic fluid so it can be considered as an oil pump. A shock absorber absorbs the road irregulaties by converting the energy. The kinetic energy that transmits from the spring converts into the thermal energy and it is dissipated with the help of hydraulic fluid inside the shock absorber. There are small holes that are located on the surface of the piston. They let the hydraulic fluid leak inside the pressure tube and this slows down general movement of the piston.

In a car with suspension system, effect of ride over rough ground is felt less. Also, it leads to improved ride quality, and increase the comfort becasue of essentially reduced degree of disturbances. Without shock absorbers, the vehicle would have a bouncing ride because the energy which is stored in the spring, is released to the vehicle and it exceeds the allowed limit of suspension movement probably. Limiting the excessive suspension movement without shock absorption requires stiffer springs, which would cause a severe ride. Soft springs could be used with shock absorbers while controlling the rate of suspension movement in response to bumps. Shock absorbers with springs usually use coil springs or leaf springs but torsion bars can be used in tensional shocks, too. However, springs are not shock absorbers. Springs store energy but do not dissipate or absorb energy. Cars are commonly equipped with springs and torsion bars as well as hydraulic shock absorbers. With this type of usage, shock absorber is allocated specifically for the hydraulic piston that absorbs and dissipates energy [8].

There are two stages in the operaion of the shock absorber. First stage is compression. In this stage piston goes down and compress the hydraulic fluid below

the piston. The second stage is the extension stage. In this stage, the piston goes to the upward compresses the hydraulic fluid above the piston. Shock absorber can be seen in Figure 2.8 [23].

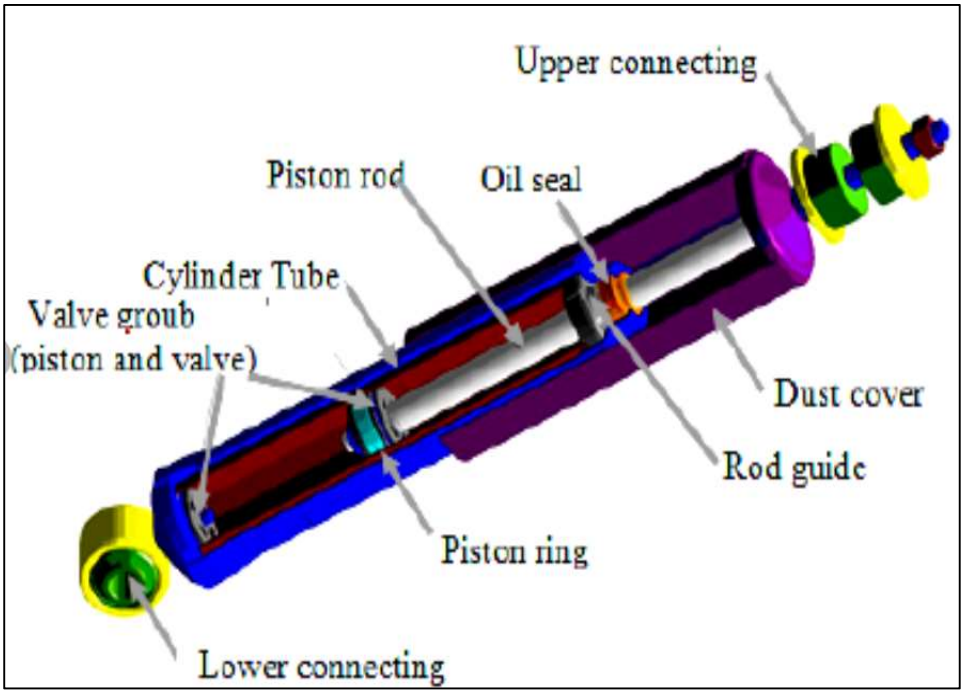

Figure 2.8: Shock absorber.

2.2.2. Anti-Sway Bar

Anti-Sway bar is as important an important part of the suspension system. Its basic duty is to connect the suspension systems to each other. At the first view, anti-sway bar looks like a dependent suspension system but that is not the case; anti-sway bars are used in independent suspension systems on all types of cars and trucks.

Anti-roll bars also called as stabilizer or sway bar. It is a rod or tube and usually made of steel. It attaches the right and left suspension members together to prevent roll or swaying of the car which occurs during cornering or due to road bumps. Vehicle anti-roll bar is part of an automobile suspension system. The bar's resistance to twist grades its ability to reduce body roll. Most of cars have front anti-roll bars. Anti-roll bars at both the front and the aft wheels can decrease roll further. If an anti-roll bar is chosen and installed correctly, it will reduce body roll and lead to better handling and increased travel comfort. Anti-Sway bar can be seen with wheels in Figure 2.9 [22].

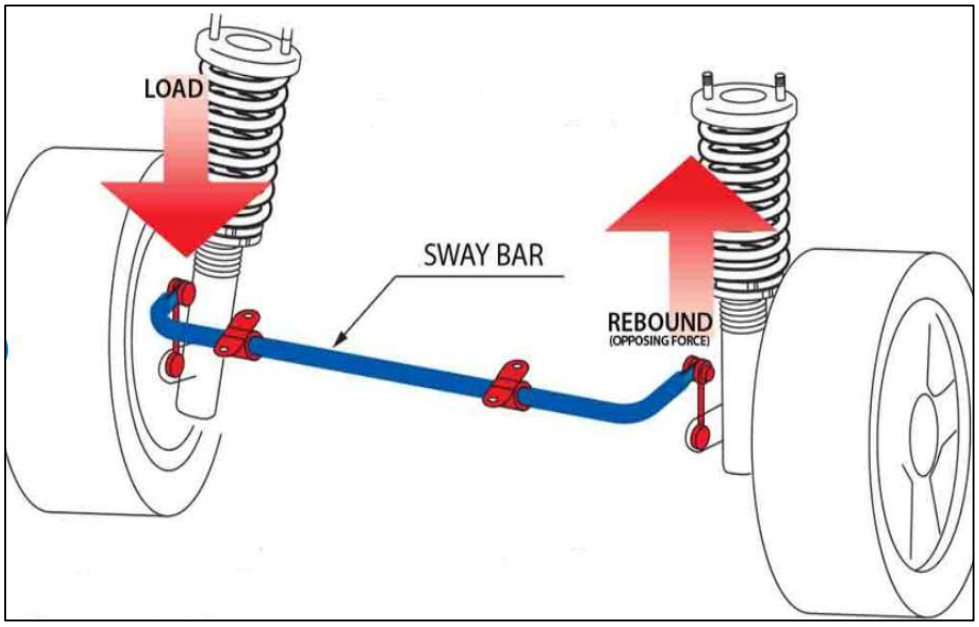

Figure 2.9: Anti-Sway bar.

2.2.3. Springs

Springs are the most important components of any suspension system. It sounds that shock absorbers absorb the bumps and shocks come from the road but this is not the case. Actually springs absorb the shock and shocks absorber convert the kinetic energy that transmitted from the road to the thermal energy. For a comfortable drive, when a car passes over a bump, the spring goes upward and will be compressed. This stored energy transmit to shock absorber piston and then is dissipated as thermal energy. The spring relax and push the wheel to the road.

Stiffness of the springs is important because it affects the response of the car while is being driven. The spring can be loosely or tightly. Loosely springs are usually used for cars, because it can swallow the bumps and provide a smooth ride. Despite its smooth ride, it is not good at cornering, braking and acceleration. When the car brakes and accelerates, drivers can feel like dive and squat. When the car corners, the body will sway or roll. Tightly springs are usually used for sports cars. They do not provide as smooth drive as luxury cars in rough roads but they are good at braking and cornering. The body does not sway or roll while cornering and braking. With this aspect, it can be said that, sport cars can be ridden aggresively.

Spring is simple but an important device and used in many areas in industry. In a car suspension system it is important how to design the spring. Because it is the most important component to provide a comfortable drive. According to type of the car, geometry and kind of spring change. Also, the material of the spring is up to the requirements of the vehicle. There are some manufacturing methods that are used to change material property of the spring and one of them is explained in this thesis.

There are three main types of springs. They are coil spring, leaf spring and torsion bar. Each of them has different characteristic and usage area. In the following sections, these types and usage areas will be explained extensively.

2.2.3.1. Coil Springs

Coil springs are also known as helical springs. Their shape is in a spiral formation. In the last few decades coil springs are widely used. For example, on MacPherson type struts, a coil spring is used with a shock absorber the other types of suspension systems, without struts, coil springs and shock absorbers are mounted seperately.

There are different kinds of springs for each kind of car and truck depending on the vehicle's suspension design, but the coil spring has a wide range of usage. Spring rate is the energy absorption capability of a spring. The spring rate is the ratio of energy absorbed; per length the spring is flexed. A coil spring is a length of elastic wire wound into coil [11].

The most important advantage of the coil spring is variable rate characteristic. To explain in detailed, some examples are given. For example, when a truck is unloaded, spring rate is loose and allows a comfortable ride. When truck is loaded, the spring rate is stiffer and increases the stability and it prevents dropping when the car pass over a bulge in the road. The other exmaple is performance-oriented cars. They have a low ride height and variable rate springs are suitable for them too. When the car drive normally, the spring provides a comfortable drive. If the car brakes, accelerates or corners the spring become a stiffer and reduce body roll.

The mostly known disadvantage of the coil springs is not to be used for vehicles that carrying heavy loads. For these type of vehicle usually leaf springs are used. Coil springs concentrate the weight of car onto a smaller surface area of the car frame because of its geometry. But leaf springs' geomerty allows to spread the vehicle weight. Some manufacturers insist on using coil springs for heavy load carrying vehicles and they have to add some speacial equipment. Some coil springs are shown in Figure 2.10 [23].

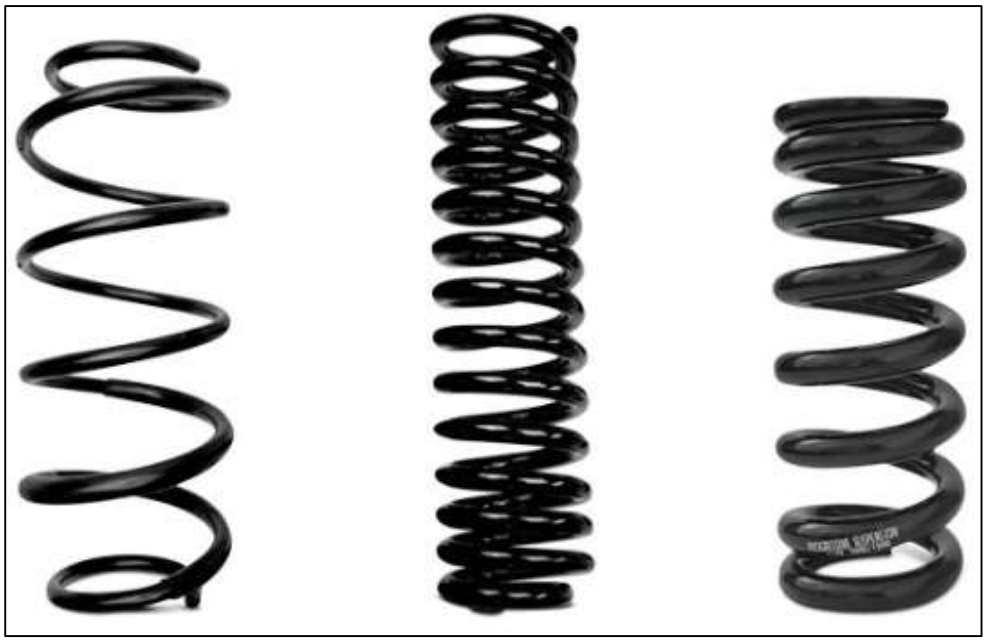

Figure 2.10: Coil springs.

2.2.3.2. Leaf Spring

Leaf springs are the oldest springs that ever known. Usage of leaf springs have started with horse-driving carriages. Its geometry is so simple and arc shaped. Usually, it is made of steel. Each of arched steel piece is named as leaf and that leaves can be stacked each other. These stacks are bonded to a solid axle beam and carry the weight of the vehicle and ensure a comfortable drive.

There are mainly 2 kinds of leaf spring. They are mono leaf and multi leaf spring. A mono leaf, as can be guessed from its name, consists of just one leaf. It is suitable for small lightweight cars. Multi leaf spring consists of multiple leaves and they are stacked up.

Leaf spring has a wide range of usage in automobiles and one of the components of suspension system. It has one or more leaves. Generally, the leaf spring must be thought as a safety component as failure could cause bad accidents. The leaf springs may carry loads, brake torque, driving torque, etc. in addition to shocks. The multi-leaf spring is made of many steel leaves of different lengths bonded to each other. The spring compresses to absorb road irregularities while driving. The leaf springs allow the suspension movement by bending and sliding on each other. [16].

Advantages of leaf springs are its simple geometry and few number of components. Also, it is simple to mount it. There are no complex suspension linkages. They are just bolted to an axle. Unlike coil springs, leaf springs propagate the load out across car's chassis and that is why it is preferred for vehicles that carries heavy loads.

Disadvantage of leaf springs is its mounting type. As mentioned before it is bolted directly to rear axles so when vehicle accelerate or brake, the torque that generated can cause axle rotate which creates vibration and uncomfortable drive. Leaf spring and its some parts can be seen from Figure 2.11 [25].

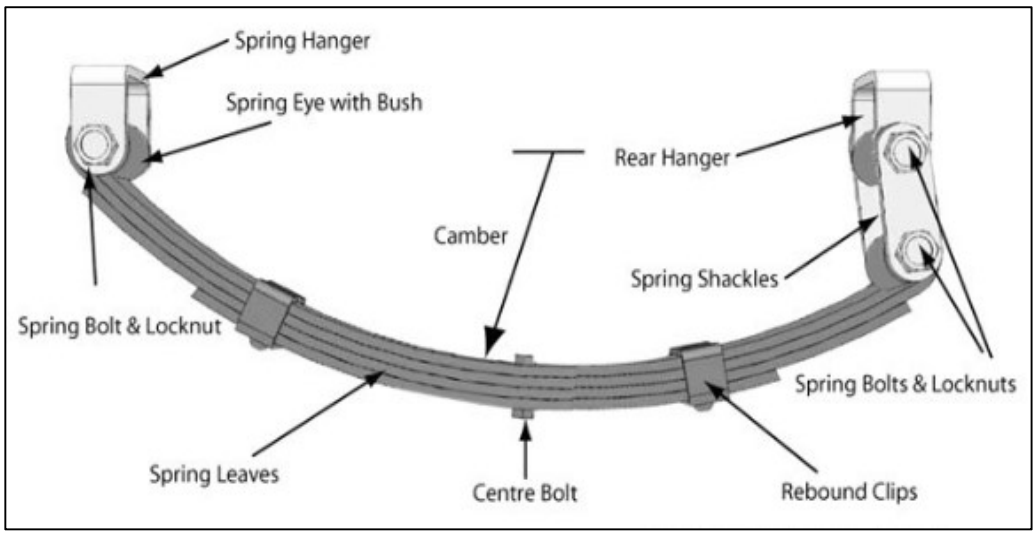

Figure 2.11: Leaf spring.

2.2.3.3. Torsion Bar

Torsion bars are different from a leaf spring or a coil spring. It can not be compressed like coil springs. It is a narrow steel tube and twists along its axis.

Although there are some wheel driven vehicles using this type of suspension, tracked vehicles usually use torsion bar as suspension equipment. The suspension works by having one end of the bar fixed in position on the car chassis to resist rotation, whilst the other end is connected to a control arm and wheel hub. The control arm is fixed to the chassis using rubber bushings which allow only vertical movement about the mounting points. There are number of splines that connects the torsion bar to the control arm. They also translate the vertical motion of the control arm into a rotational or torsional force [18].

Torsion bars' the most important advantage is to take up less space than other suspension systems. Also it is cheap so the car manufacturers prefer torsion bars mostly. The other important advantage of torsion bar is that it allows adjusting the ride height. It can be easily adjusted to owner's taste.

Torsion bars' disadvantage is to be bonded low along the vehicle's underside. They are vulnerable to external effects. When the car pass over bumps or rough roads, it can be damage more easily. It is essential to visually survey them for damage in the event they have become bent, scraped, or cracked. Torsion bar and its mounting can be seen in Figure 2.12 [25].

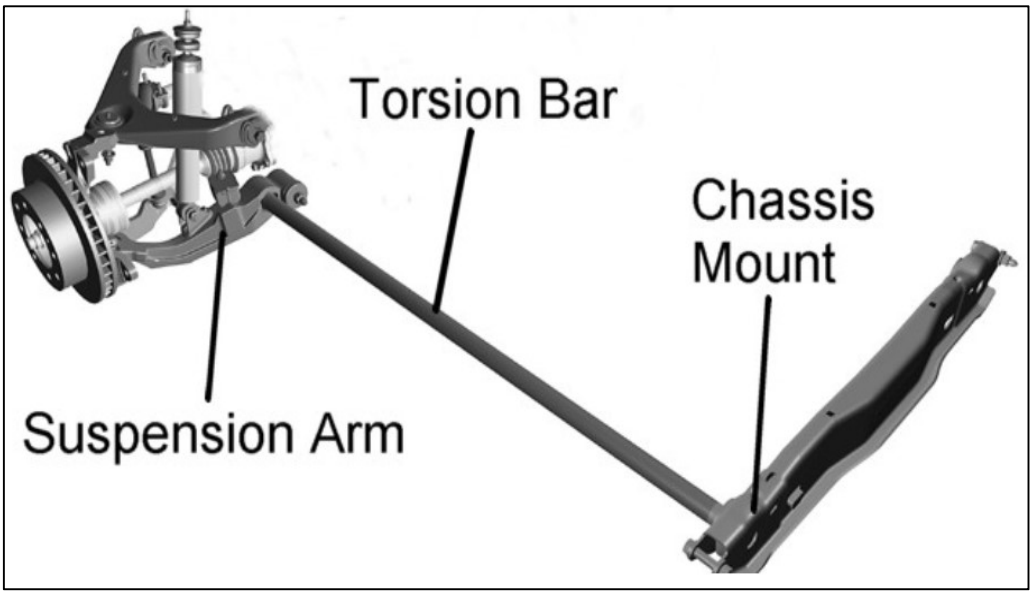

Figure 2.12: Torsion bar.

2.2.3.4. Pigtail Spring

Pigtail springs are two types. First type is single pigtail springs that have one flat end and one pigtail end. Second type is double pigtail springs that have two pigtail ends. The pigtails usually have different diameters and coils' ends have different angles. Also, pigtail spring's coil diameter can be arranged so its coils can fit into each other even for short length compression. This geometric solution can decrease the bloc length close to two times the material's diameter. This decreased, very small bloc length of the spring leads to less requirement of space and this an advantage. This advantage can be useful in the rear of a car when, for instance, a flat loading area is required. The kind of the material, like tapered or parallel, is not important for fitting of coils inside each other, because it is dependent on the diameter of the coils. Although tapered material is sometimes used to save weight for this design, premature end coil can be existed. A linear load and deflection characteristics can be achieved for pigtail springs with the use of 2 kinds of the materail like tapered or parallel wire. They mostly have a progressive or linear characteristic because the decreased material diameter compensates for the reduction in the springs external diameter. Double pigtail spring is shown in Figure 2.13 [26].

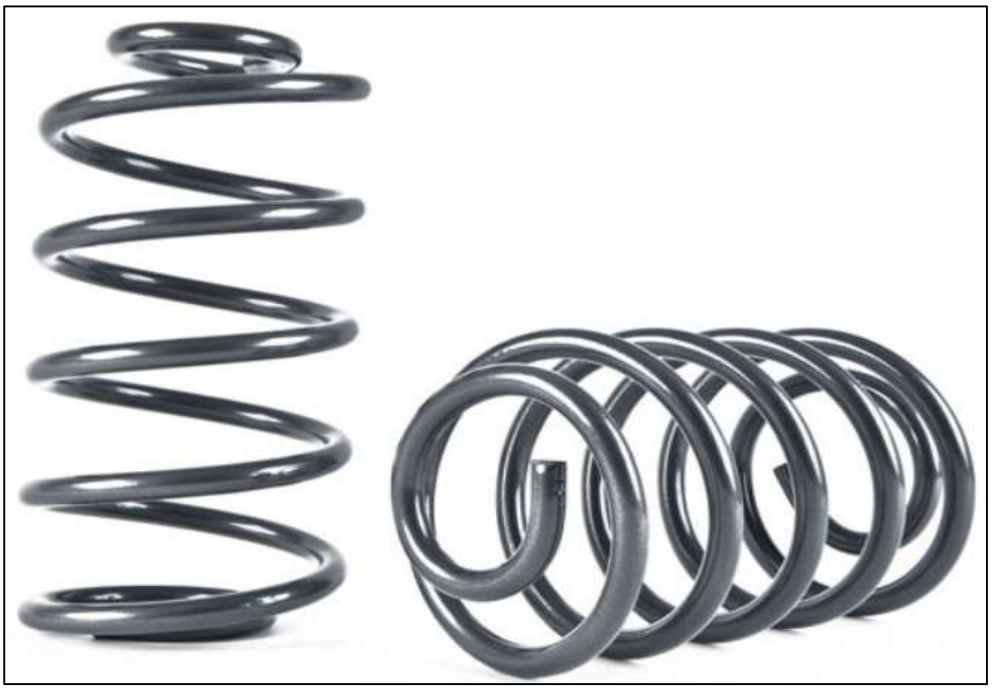

Figure 2.13: Double pigtail spring.

Other type of pigtail spring is single pigtail spring and shown in Figure 2.14 [26].

Figure 2.14: Single pigtail spring.

3. SPRINGS USED IN THE STUDY

3.1. Spring Models

In this study, it is collaborated with Rözmaş company. The company is established in 1991 and has 20 years experience in manufacturing stabilizer bars and coil springs, certificated with ISO TS 16949 since 2003. The company has its own design team and test equipments. Spring and stabilizer bars are can be designed and tested with test machines at the headquarter in Gebze. The pigtail spring is used in the study because of the firm demand. Four different spring models are analysed. The models are prepared by Catia by the firm design team. The firm has its own name coding system for springs and these names are used in this study.

3.1.1. 2319 Model Spring

2319 model spring's 3D geometry is shown in Figure 3.1.

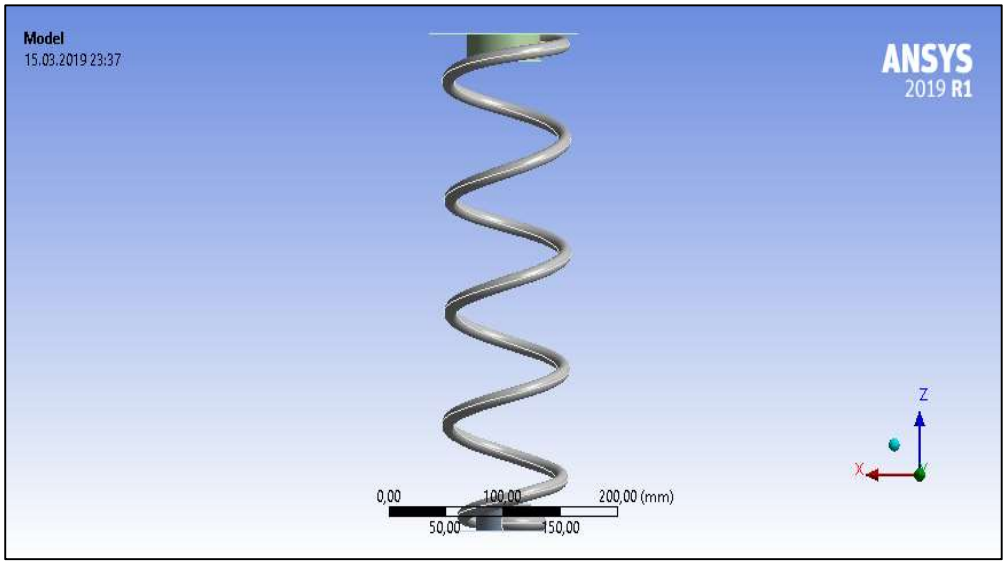

Figure 3.1: 2319 model spring 3D geometry.

2319 model spring's main dimensions are shown in Table 3.1.

Table 3.1: Properties of 2319 model spring.

Spring Length (mm)	366.22
Wire Diameter (mm)	10.7
Coil Diameter (mm)	109.727

3.1.2. 2299A Model Spring

2299A model spring's 3D geometry is shown in Figure 3.2.

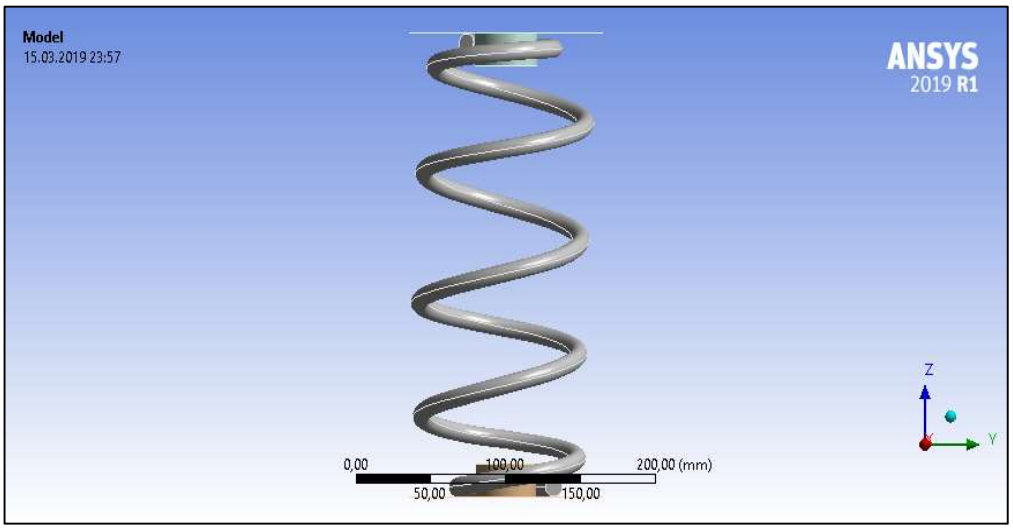

Figure 3.2: 2299A model spring 3D geometry.

2299A model spring's main dimensions are shown in Table 3.2.

Table 3.2: Properties of 2299A model spring.

Spring Length (mm)	282.4
Wire Diameter (mm)	11.25
Coil Diameter (mm)	114.23

3.1.3. 2309 Model Spring

2309 model spring's 3D geometry is shown in Figure 3.3.

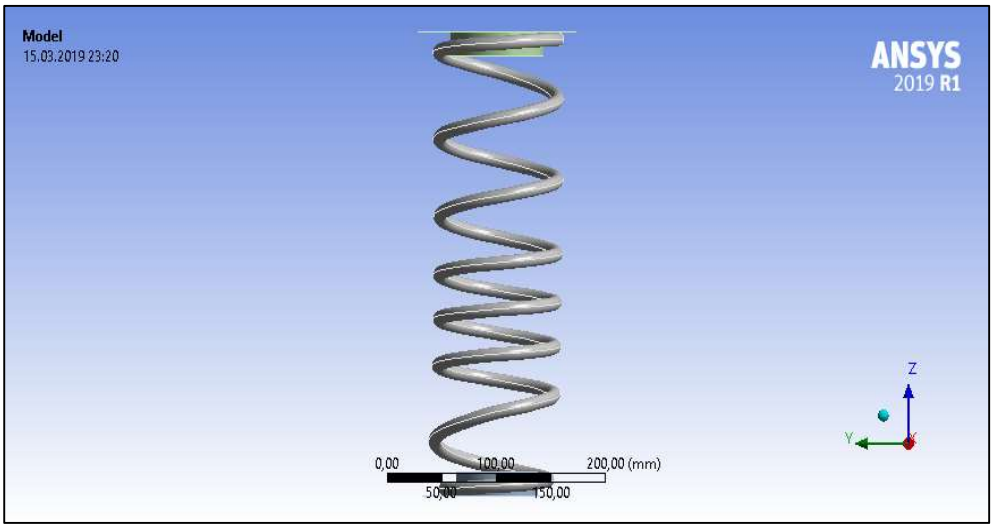

Figure 3.3: 2309 model spring 3D geometry.

2309 model spring's main dimensions are shown in Table 3.3.

Table 3.3: Properties of 2309 model spring.

Spring Length (mm)	380.06
Wire Diameter (mm)	11.5
Coil Diameter (mm)	118.2

3.1.4. 2304A Model Spring

2304A model spring's 3D geometry is shown in Figure 3.4.

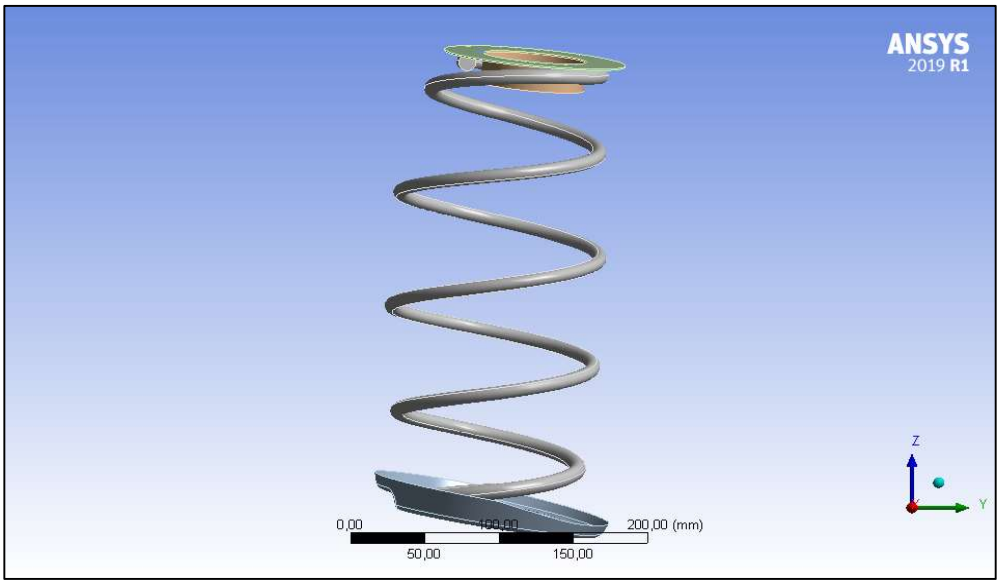

Figure 3.4: 2304A model spring 3D geometry.

Coil diameter of 2304A spring is changing along its axis and mean coil diameter is shown in table 3.1. Also, spring's centerline axis direction and force centerline direction are different and angle between these axis is 5.56 degree. The properties of lower plate is shown in Figure 3.5 and axis of spring is shown in Figure 3.6.

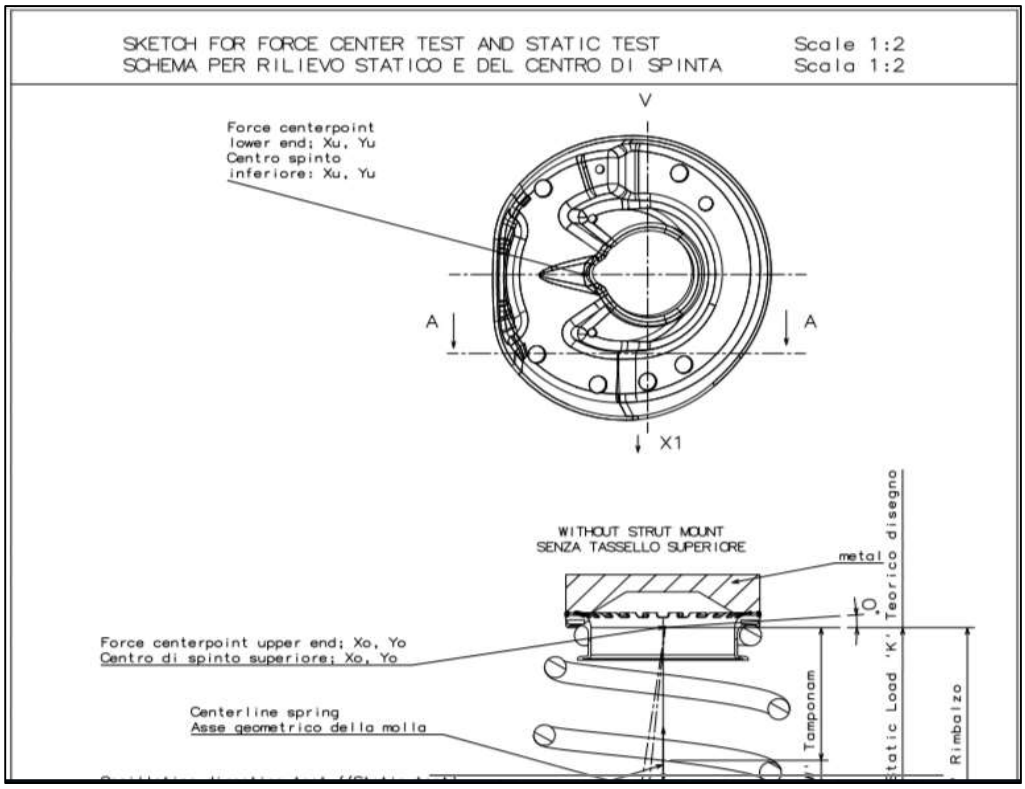

Figure 3.5: Lower plate of 2304A model spring.

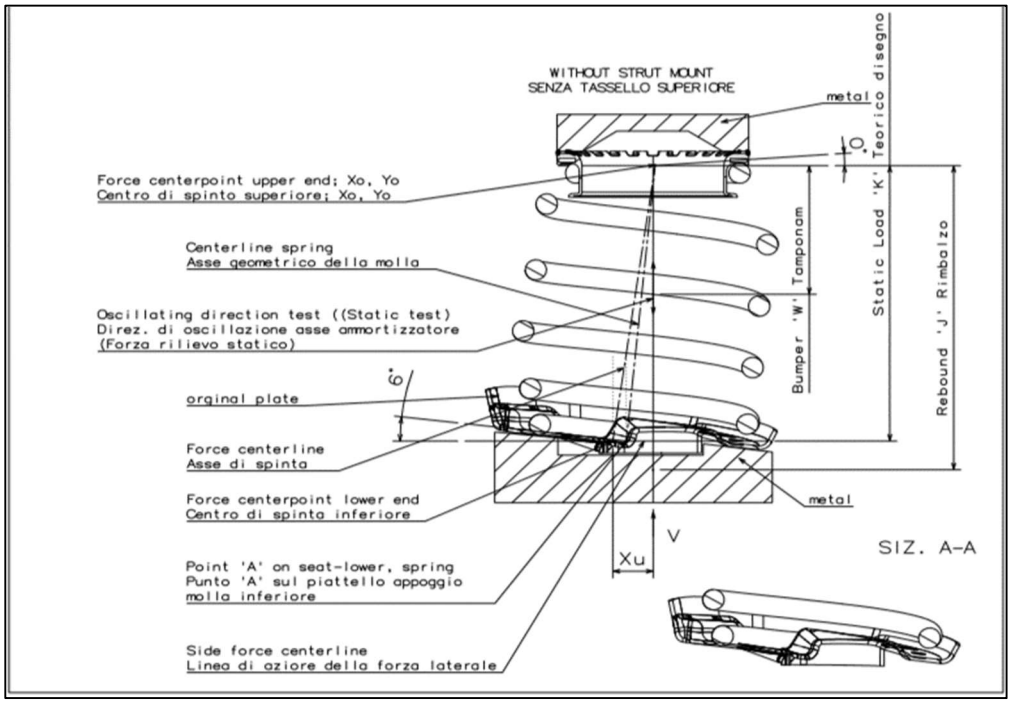

Figure 3.6: Geometry of 2304A model spring.

Force center point of upper end and lower end is shown in Table 3.4.

Table 3.4: Force center point of ends of 2304A model spring.

Force center point upper end	Xo	[mm]	0±5
	Yo	[mm]	0±5
Force center point lower end	Xu	[mm]	-30±5
	Yu	[mm]	0±5

2309 model spring's main dimensions are shown in Table 3.3.

Table 3.5: Properties of 2304A model spring.

Spring Length (mm)	327
Wire Diameter (mm)	11.9
Max. Coil Diameter (mm)	129.33

4. ANALYSIS OF SPRINGS

4.1. Analysis Types Used For Spring Models

In this study, four analyses types are used. The methods are static structural (Large deflection off and Large deflection on), transient structural (implicit) analyse and workbench LS-DYNA (explicit). The analyses types, which are used, are explained in the following section.

4.1.1. Static Structural Analysis

In a static structual analysis loading and response conditions are assumed steady and it means that both the loads and response vary slowly with respect to time. Also, significant inertia and damping effects are not included in the static structural analysis. It means that loads are applied without inertia and damping effect and result in the displacements, stresses, strains, and forces in structures or components [27].

The explanation above is valid for all degrees of freedom (dofs). Inertial and damping effects are not included except for static acceleration fields [2].

The overall equilibrium equations for linear structural static analysis are:

$$[K]\{u\} = \{F\} \tag{4.1}$$

or

$$[K]\{u\} = \{Fa\} + \{Fr\} \tag{4.2}$$

- [K] : total stiffness matrix = $\sum_{m=1}^{N}$[Ke]
- {u} : nodal displacement vector
- N : number of elements
- [Ke] : element stiffness matrix
- {Fr} : reaction load vector

{Fa}, the total applied load vector, is defined by:

$$\{Fa\} = \{Fnd\} + \{Fac\} + \sum_{m=1}^{N} (\{Feth\} + \{Fepr\}) \tag{4.3}$$

- {Fnd} : applied nodal load vector
- {Fac} : -[M]{ac}=acceleration load vector
- [M] : total mass matrix = $\sum_{m=1}^{N}$[Me]
- [Me] : element mass matrix
- {ac} : total acceleration vector
- {Feth} : element thermal load vector
- {Fepr} : element pressure load vector

In equation (4.1), {F} is statically applied. There are no inertial effects (mass, damping). Also, time-varying forces are not considered. [K] is constant because linear elastic material behavior is assumed and small deflection theory is accepted.

It is important to that these assumptions are valid for linear static analysis. For nonlinear static analysis, "Large Deflection On" is activated in the "Analysis Settings" details and so strain term is changed.

Small value of strains in a material can be neglected but if the strains in a material exceeding more than a few percent can not be neglected. Because this deformation leads to change in geometry. Analyses which include this effect are called large strain, or finite strain, analyses. In a static or transient analysis large strain analysis can be run if large deformation effect is opened and the suitable element type is used. Large strain formulation is also valid for elastic-plastic elements. This kind of elements use a hypoelastic formulation so that they are restricted to small elastic strains but allow for arbitrarily large plastic strains. On the other hand, hyperelasticity addresses the large strain formulation for hyperelastic elements, that allow arbitrarily large elastic strains [2].

The large strain theory is based on a few basic pysical quantities, for example motion and deformation, and the regarding mathematical relationship. The load that is applied on a body make it move from one position to another. This motion can be explained by working on a position vector in the "deformed" and "undeformed"

configuration. Say the position vectors in the “deformed” and “undeformed” state are shown by {x} and {X} respectively, then the motion vector {u} is computed by;

$$\{u\} = \{x\} - \{X\} \tag{4.4}$$

Position vectors and motion of a deforming body is shown in Figure 4.1 [2].

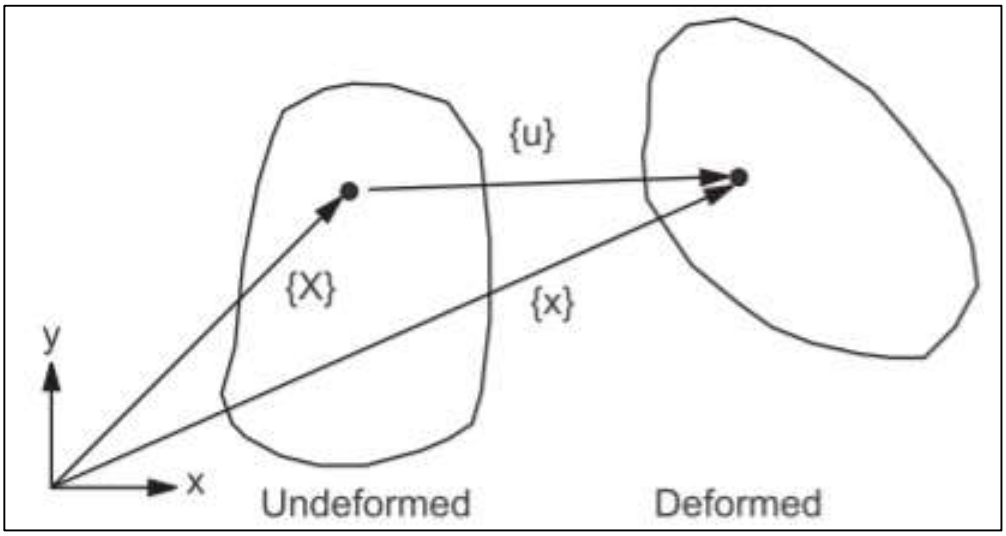

Figure 4.1: Position vectors and motion of a deforming body.

The deformation gradient is defined as:

$$[F] = \partial\{x\}/\partial\{X\} \tag{4.5}$$

which can be shown in terms of the displacement of the point by equation (4.4) as:

$$[F] = [I] + \partial\{x\}/\partial\{X\} \tag{4.5}$$

where:

[I]: identity matrix

The information contained in the deformation gradient [F] includes the volume change, rotation and the shape change of the deforming body. The changing volume at a point is shown by equation (4.6):

$$det[F] = dV/dVo \tag{4.6}$$

where:

- Vo: original volume
- V: current volume
- det[ ]: determinant of the matrix

The deformation gradient can be separated into a rotation and a shape change using the right polar decompostion theorem:

$$[F] = [R][U] \tag{4.7}$$

where:

- [R]: rotation matrix ($[R]^T[R]=[I]$)
- [U]: right stretch (shape change) matrix

Once the stretch matrix is known, a logarithmic or Hencky strain measure is defined as:

$$[\varepsilon] = ln[U] \tag{4.8}$$

[ε] is in tensor (matrix) form here, as opposed to the usual vector form {ε}. Since [U] is a second order tensor (matrix), equation (4.8) is determined by the spectral decomposition of [U]:

$$[\varepsilon] = \sum_{i=1}^{3} ln\, \lambda i\{ei\}\{ei\}^{T} \tag{4.9}$$

where:

- λi: eigenvalues of [U] (principal stretches)
- {ei}: eigenvectors of [U] (principal directions)

The polar decomposition theorem equation (4.7) extracts a rotation [R] that represents the average rotation of the materail at a point. Material lines initially orthogonal will not, in general, be orthogonal after deformation (because of shearing). The polar decomposition of this deformation, however, will indicate that they will remain orthogonal (lines x-y' in Figure 4.2: Polar Decomposition of a Shearing Deformation [2]). For this reason, non-isotropic behavior (e.g. orthotropic elasticity or kinematic hardening plasticity) should be used with care with large strains, especially if large shearing deformation occurs [2].

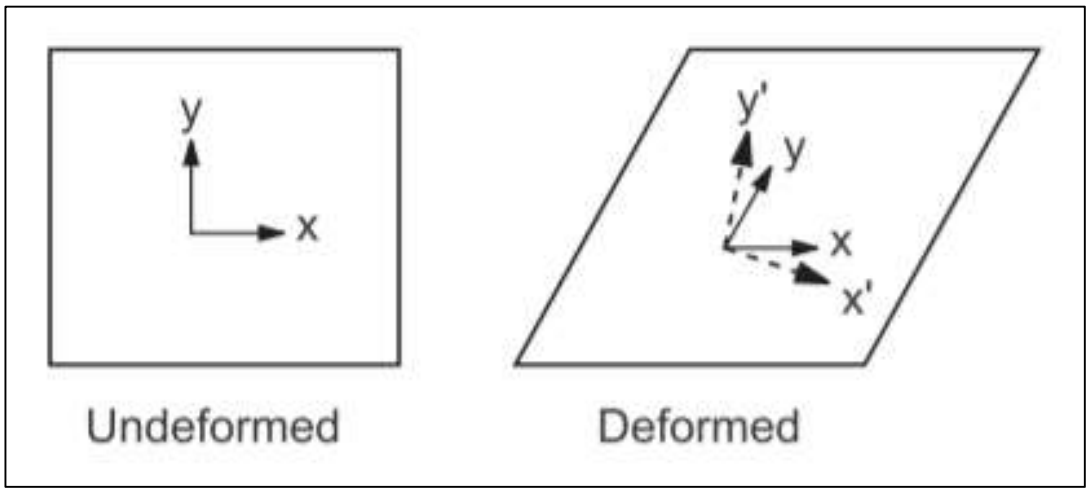

Figure 4.2: Polar decomposition of a shearing deformation.

4.1.2. Transient Structural Analysis

The method of transient analysis solution is depends on the dofs that are involved. Structural, acoustic, and other second order systems (that is, the systems are second order in time) are solved using one method and the thermal, magnetic, electrical and other first order systems are solved using another. If both first and second order dofs are included in the analysis (e.g. structural and magnetic), then each dof is solved by

using the suitable method. For matrix coupling between first and second order effects such as for piezoelectric analysis, a combined procedure is used [2].

The transient dynamic equilibrium equation of interest is like below for a linear structure [2]:

$$[K]\{u\} + [M]\{\ddot{u}\} + C\{\acute{u}\} = \{Fa\} \tag{4.10}$$

where:

- [M]: structural mass matrix
- [C]: structural damping matrix
- [K]: structural stiffness matrix
- $\{\ddot{u}\}$: nodal acceleration vector
- $\{\acute{u}\}$: nodal velocity vector
- $\{u\}$: nodal displacement vector
- $\{Fa\}$: applied load vector

There are two methods in the ANSYS program which could be used for the solution of equation (4.10) the central difference time integration method and the Newmark time integration method (including an improved algorithm called HHT). The central difference method is used for explicit transient analyses and it is described in the LS-DYNA Theoretical Manual. For implicit transient analyses the Newmark method and HHT method are used [2].

4.1.3. Ansys LS-DYNA

Ansys LS-DYNA is capable of simulating the response of materails to loading that is applied for short periods of time. It is widely used as explicit simulation program. It is capable of solving complex problems because it has many elements, contact formulations, material models and other controls over all the details of the problem [7].

Ansys LS-DYNA has its explicit solver and a huge array of capabilities so it can solve extreme deformation problems. Moreover, simulations which involves material failure can be solved. The designer can view how the failure progresses through a part or through a system. Large amounts of parts included model or surfaces comtacting with each other are also easily solved. Interactions and load passing between complex behaviors are modeled accurately. With higher numbers of CPU cores computers can solve the problem in short times [7].

Consider the single degree of freedom damped system in Figure 4.3 [7].

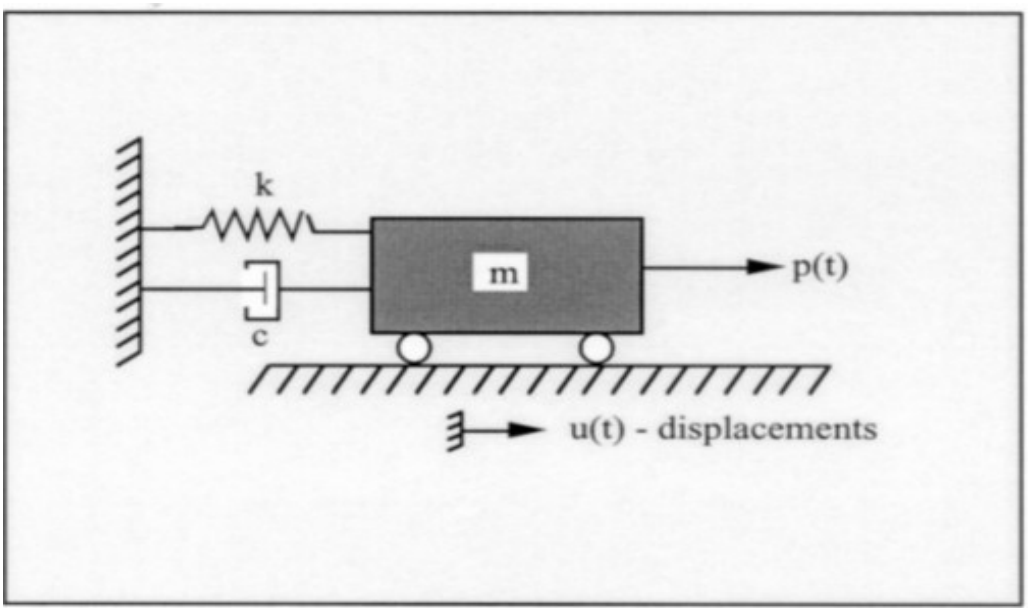

Figure 4.3: Single degree of freedom damped system.

Forces acting on mass m are shown in Figure 4.4 [7].

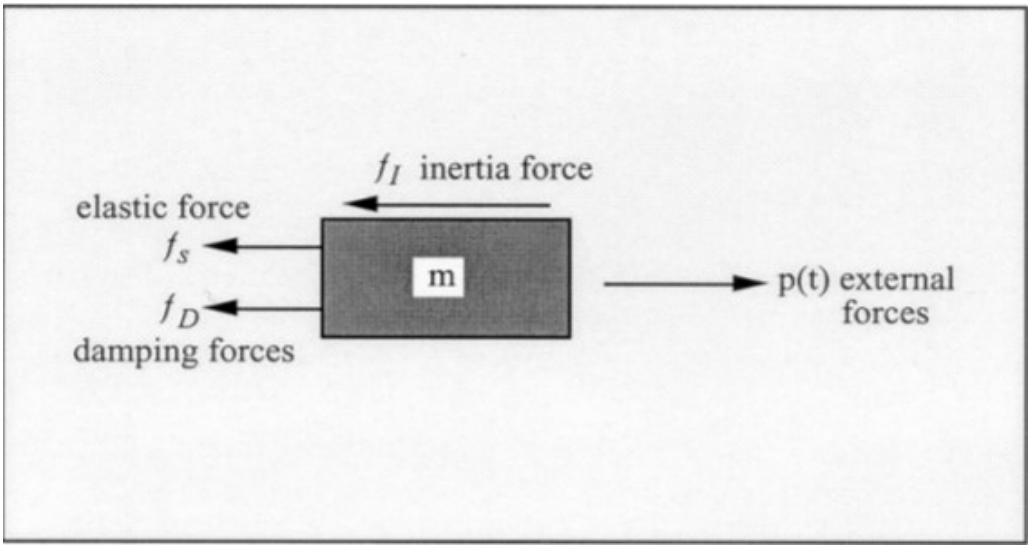

Figure 4.4: Forces acting on mass, m.

The equations of equilibrium are obtained from d'Alembert's principle [7],

$$f\imath + fD + fint = p(t) \tag{4.11}$$

$$f\imath = m\ddot{u} \tag{4.12}$$

$$fD = c\dot{u} \tag{4.13}$$

$$fint = ku \tag{4.14}$$

For critical damping $c=c_{cr}$, the equations of motion for linear characteristic result in a linear ordinary differential equation, o.d.e [7]:

$$m\ddot{u} + C\dot{u} + ku = p(t) \tag{4.15}$$

yet for the nonlinear situation the internal force changes as a nonlinear function of the displacement, resulting in a nonlinear o.d.e [7]:

$$fint(u) + m\ddot{u} + C\dot{u} = p(t) \tag{4.16}$$

Analytical solutions of linear ordinary differential equations are available, so instead the dynamic response of linear system subjected to harmonic loading is considered. It is appropriate to define some widely used terms [7]:

Harmonic loading:

$$p(t)=p_0 \sin\varpi t \tag{4.17}$$

Circular frequency:

$$\omega = \sqrt{k}/m \tag{4.18}$$

Natural frequency:

$$f=\omega/2n=1/T \tag{4.19}$$

Damping ratio:

$$\xi=c/cr=c/2m\omega \tag{4.20}$$

Damped vibration frequency:

$$\omega_0=\omega\sqrt{1-\xi^2} \tag{4.21}$$

Applied load frequency:

$$\beta=\varpi/\omega \tag{4.22}$$

The closed form solution is [7]:

$$u(t) = u0coswt + \left(\frac{\acute{\upsilon}0}{w}\right) sinwt + \left(\frac{p0}{k}\right)\left(\frac{1}{1-\beta^2}\right)(sin\varpi t - \beta sinwt) \tag{4.23}$$

Just numerical solutions are possible for nonlinear problems. Explicit central difference scheme is used to integrate the equations of motion in LS-DYNA [7].

4.2. Analysis of Spring Models

All spring models are made of 54SiCr6 (Silicon-Chromium Steel). It is hot rolled steel for quenched and tempered. It is produced by cold and hot forming. The chemical composition of the material is shown in Table 4.1. The properties of the spring material is shown in Table 4.2. The stress and strain graph that are obtained from the material tensile test is shown in Figure 4.5.

Table 4.1: The chemical composition of the material.

C	Si	Mn	P	S	Cr
0.56	1.45	0.70	<0.01	<0.01	0.65

Table 4.2: The properties of the spring material.

Elasticity Module (MPa)	Poisson Ratio	Yield Strength (MPa)	Ultimate Strength (MPa)
206000	0.3	1700	2000

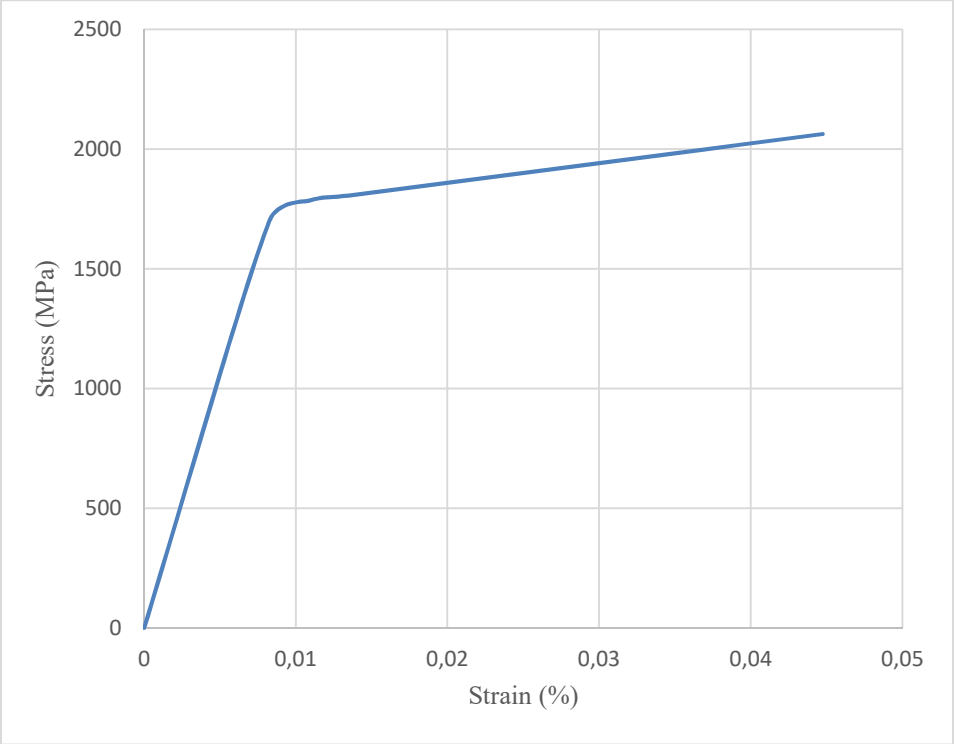

Figure 4.5: Stress - strain graph of 54SiCr6.

Plastic stress and strain values of spring material (54SiCr6) are shown in Table 4.3. Bilinear isotropic hardening method is chosen to define the plastic region of the material and tangent modulus is 8163 MPa.

Table 4.3: Plastic stress-strain values of the spring material.

Plastic Strain (%)	Stress (MPa)
0	1700
0.0026	1785
0.0052	1806
0.0078	1827
0.0104	1849
0.0130	1870
0.0156	1892
0.0182	1913
0.0208	1935
0.0234	1956
0.0260	1977
0.0286	1999
0.0312	2020
0.0338	2042
0.0364	2063

The plates are rigid so in the analysis the plates material's property is defined as Table 4.4 for static structural analysis and transient structural (implicit) analysis. In the LS-DYNA (Explicit), plate materials are defined as rigid.

Table 4.4: The properties of the plate material.

Elasticity Module (MPa)	Poisson Ratio	Yield Strength (MPa)	Ultimate Strength (MPa)
2060000	0.3	17000	20000

The analysis are made by Ansys Workbench 2019R. The convergence is achieved with 5 mm mesh element size for all spring models. Contact types for static structural and transient stuctural analyse are the same. Spring and plates are contact during the test so in the analyses (static structural and transient structural) "Bonded" contact is defined between plates and spring. The contacts (target and contact) are shown in Figure 4.6 & 4.7.

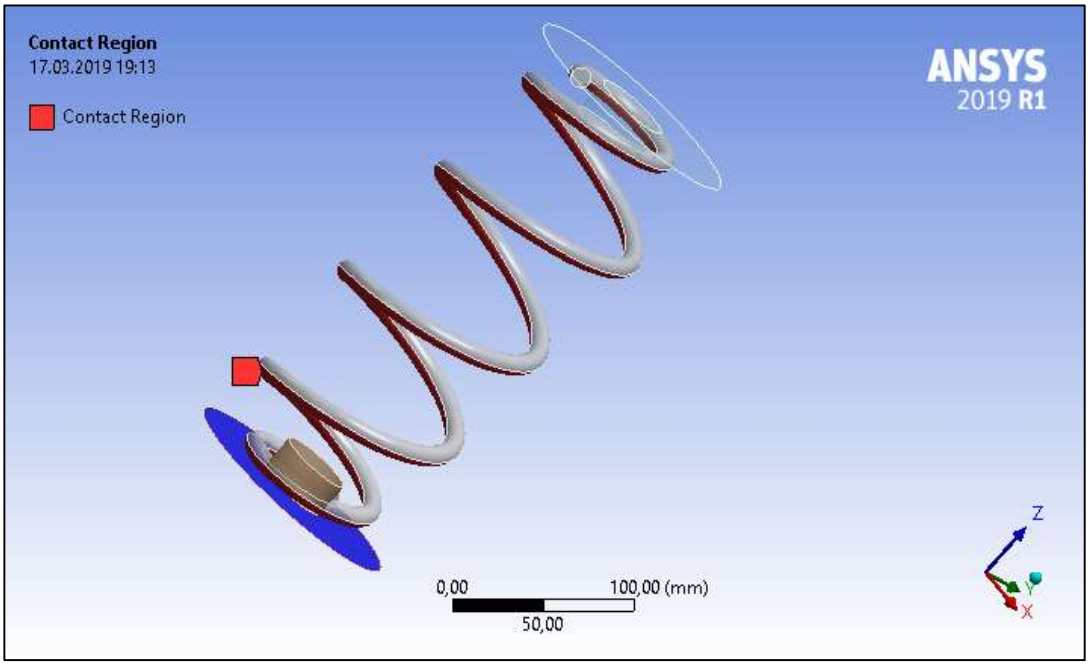

Figure 4.6: Contact region of springs.

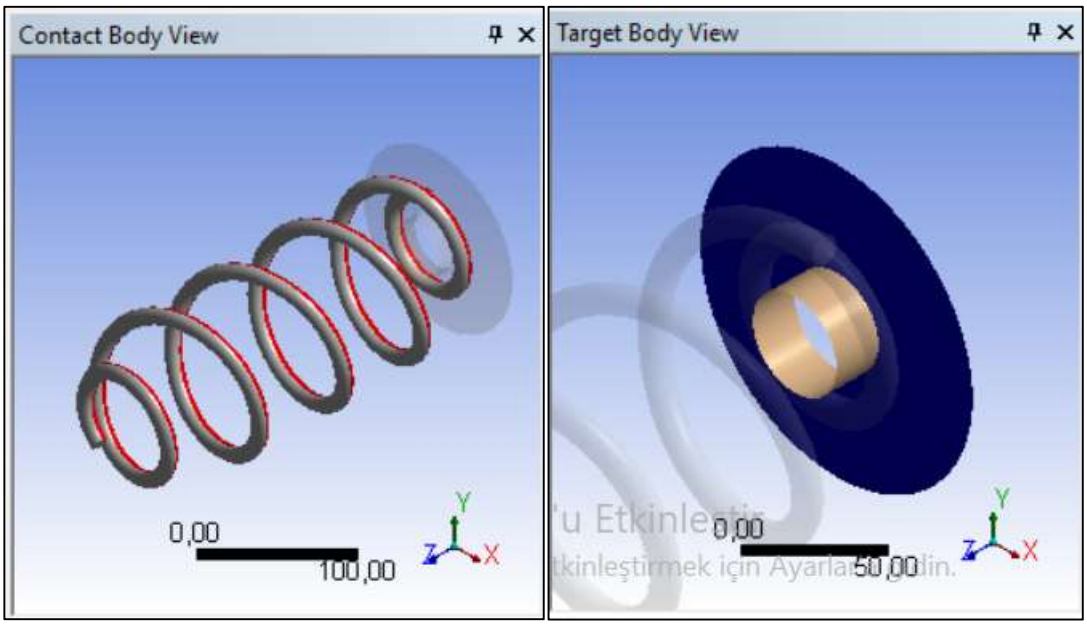

Figure 4.7: Target and contact region between spring and plate.

In workbench LS-DYNA, no contact definition is needed. “Body interaction” is enough for the analyse. In the “Details of Body Interaction”, scope is “All geometry”, type is “Frictional”, friction coefficient is “0.3” and damping factor is “0.2” as shown in Figure 4.8.

Details of "Body Interaction"	
Scope	
Scoping Method	Geometry Selection
Geometry	All Bodies
Definition	
Type	Frictional
Friction Coefficient	0,3
Dynamic Coefficient	0,2
Decay Constant	0,
Suppressed	No

Figure 4.8: Details of Body Interaction in LS-DYNA.

Boundary conditions and results for each spring model are explained in the following sections. Each spring model is analysed by 4 method and results are shown in tables. The methods are:

- Static Structural (Large Deflection Off)
- Static Structural (Large Deflection On)
- Transient Structural (Implicit)
- LS-DYNA (Explicit)

4.2.1. Analysis of 2319 Model Spring

For 2319 model spring the element size, element number and node number are shown in Table 4.5.

Table 4.5: The element size, element number and node number of 2319 model spring.

Element Size (mm)	Element Number	Node Number
5	2306	9051

2319 model spring mesh view is shown in Figure 4.9.

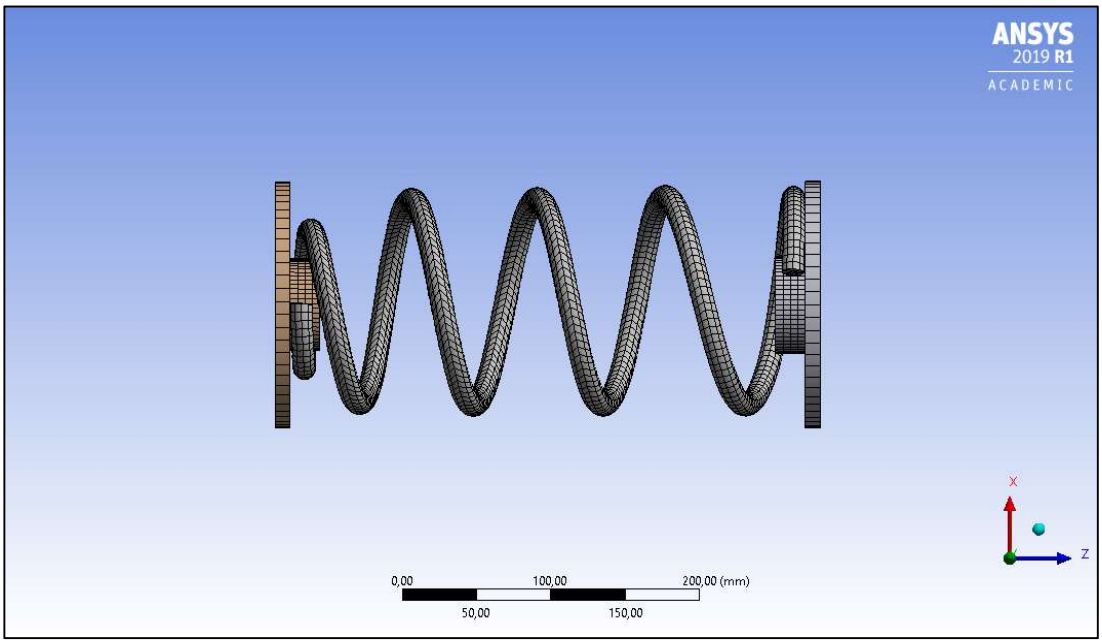

Figure 4.9: Mesh view of 2319 model spring.

Three different cases are analysed. For static structural analyse, boundary conditions that are applied on upper and lower plates are shown in the Table 4.6.

Table 4.6: Boundary conditions for static structual analyse of 2319 model spring.

Cases	Lower plate	Upper plate
Case 1	Fixed Support	Displacement, -z, 126.22 mm
Case 2	Fixed Support	Displacement, -z, 160.22 mm
Case 3	Fixed Support	Displacement, -z, 176.22 mm

For transient structural analyse, boundary conditions that are applied on upper and lower plates are shown in the Table 4.7.

Table 4.7: Boundary conditions for transient structual analyse of 2319 model spring.

Cases	Lower plate	Upper plate	Step End Time
Case 1	Fixed Support	Velocity, -z, 10 mm/s	12.622 s
Case 2	Fixed Support	Velocity, -z, 10 mm/s	16.022 s
Case 3	Fixed Support	Velocity, -z, 10 mm/s	17.622 s

For workbench LS-DYNA (Explicit) analyse, boundary conditions that are applied on upper and lower plates are shown in the Table 4.8.

Table 4.8: Boundary conditions for LS-DYNA (Explicit) analyse of 2319 model spring.

Cases	Lower plate	Upper plate
Case 1	Rigid Body Constraint, All fixed	Displacement, -z, 126.22 mm
Case 2	Rigid Body Constraint, All fixed	Displacement, -z, 160.22 mm
Case 3	Rigid Body Constraint, All fixed	Displacement, -z, 176.22 mm

The 2319 model spring is analysed and the results for 126.22 mm applied displacement are shown in Table 4.9.

Table 4.9: Comparison of calculated reaction forces for applied displacement 126.22 mm.

Analysis Type	Achieved Displacement (mm)	Reaction Force (N)	Reaction Force (Experimental) (N)
Static(Large Deflection Off)	126.33	3426.1	2903
Static(Large Deflection On)	126.33	3277.8	2903
Transient (Implicit)	126.33	3280.1	2903
LS-DYNA (Explicit)	126.81	2878.5	2903

2319 model spring is analysed by static & transient method and total deformation under 126.22 mm displacement is shown in Figure 4.10.

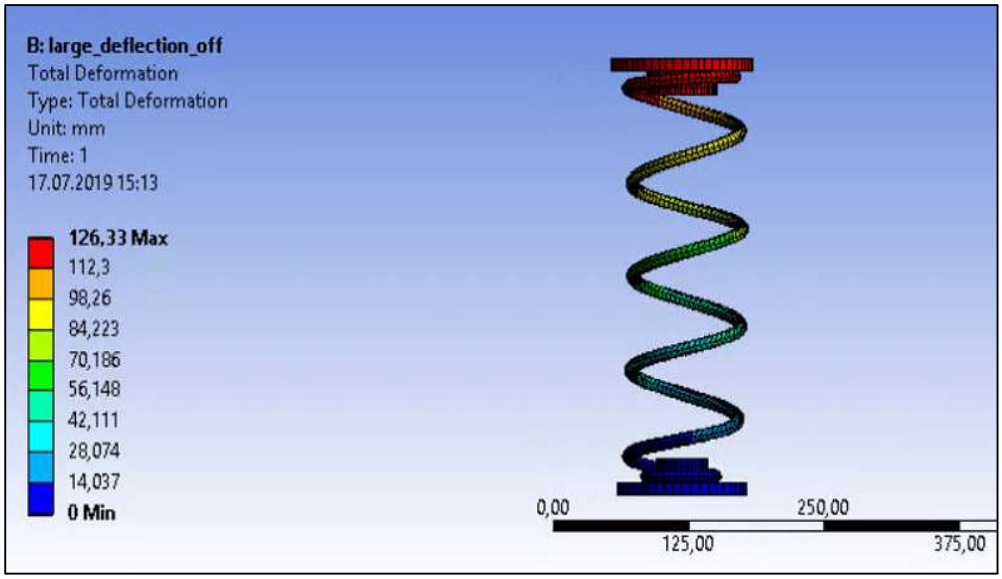

Figure 4.10: Total deformation of 2319 model spring under 126.22 mm displacement, Ansys (Static & Transient) analysis.

2319 model spring is analysed by LS-DYNA method and total deformation under 126.22 mm displacement is shown in Figure 4.11.

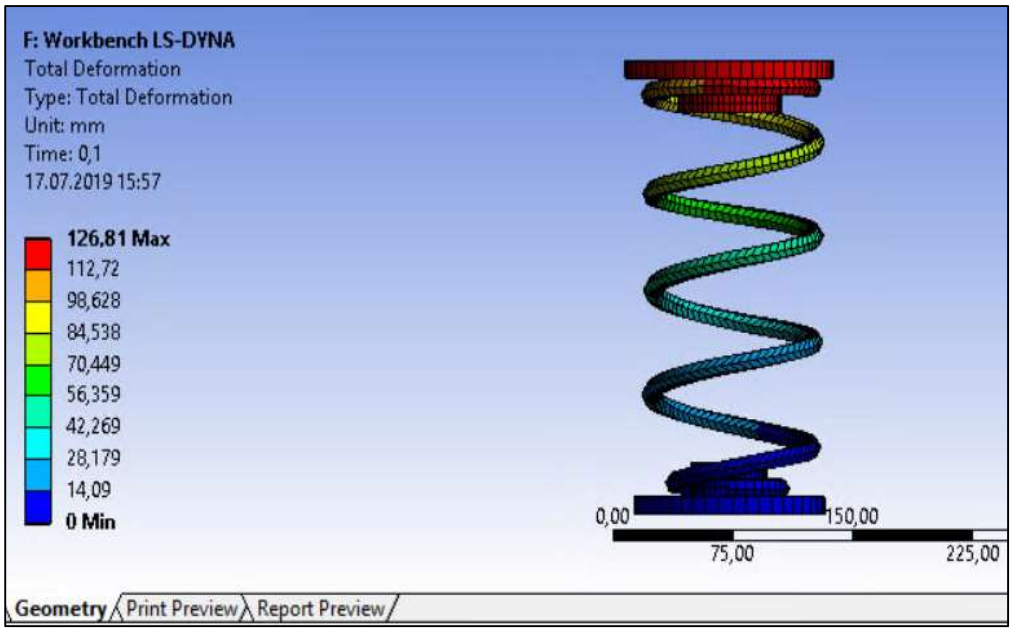

Figure 4.11: Total deformation of 2319 model spring under 126.22 mm displacement, LS-DYNA analysis.

The 2319 model spring is analysed and the results for 160.22 mm applied displacement are shown in Table 4.10.

Table 4.10: Comparison of calculated reaction forces for applied displacement 160.22 mm.

Analysis Type	Achieved Displacement (mm)	Reaction Force (N)	Reaction Force (Experimental) (N)
Static(Large Deflection Off)	160.36	4340.5	3666
Static(Large Deflection On)	160.36	4124.1	3666
Transient (Implicit)	160.36	4248.5	3666
LS-DYNA (Explicit)	160.40	3690.5	3666

2319 model spring is analysed by static & transient method and total deformation under 160.22 mm displacement is shown in Figure 4.12.

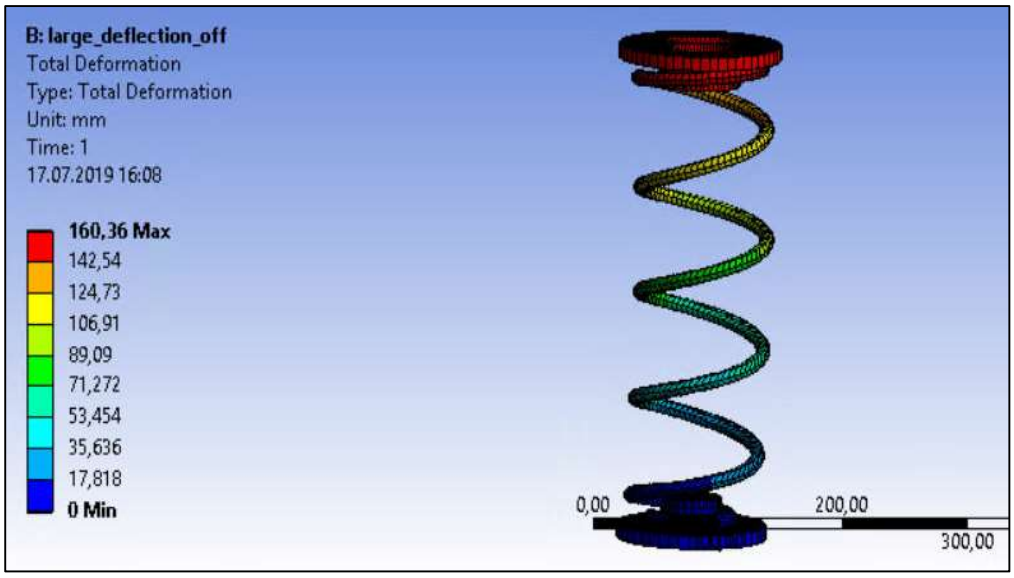

Figure 4.12: Total deformation of 2319 model spring under 160.22 mm displacement, Ansys (Static & Transient) analysis.

2319 model spring is analysed by LS-DYNA method and total deformation under 160.22 mm displacement is shown in Figure 4.13.

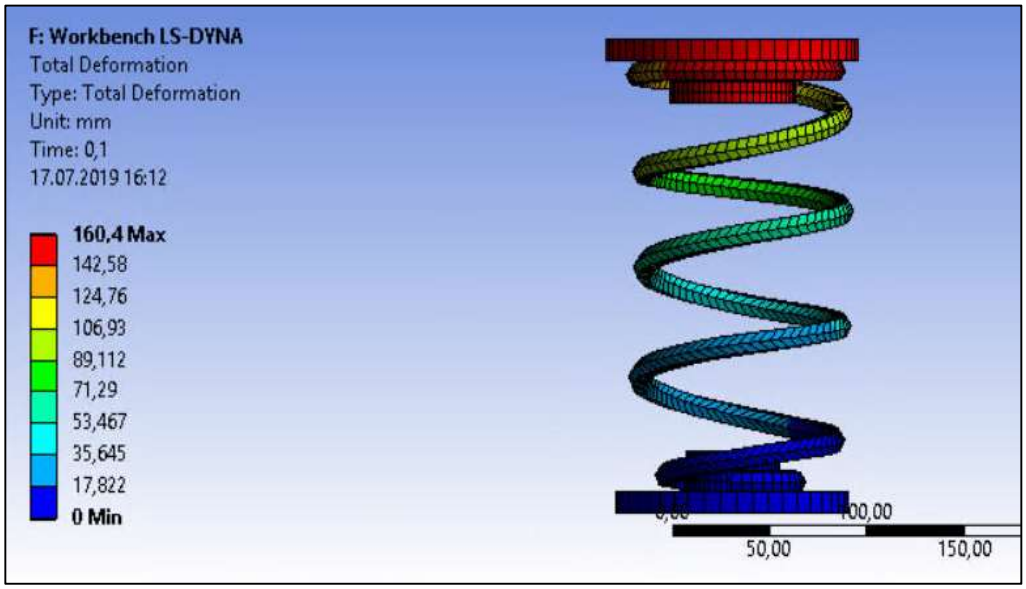

Figure 4.13: Total deformation of 2319 model spring under 160.22 mm displacement, LS-DYNA analysis.

The 2319 model spring is analysed and the results for 176.22 mm applied displacement are shown in Table 4.11.

Table 4.11: Comparison of calculated reaction forces for applied displacement 176.22 mm.

Analysis Type	Achieved Displacement (mm)	Reaction Force (N)	Reaction Force (Experimental) (N)
Static(Large Deflection Off)	176.38	4772.9	4022
Static(Large Deflection On)	176.38	4501.8	4022
Transient (Implicit)	176.38	4499.9	4022
LS-DYNA (Explicit)	176.32	4260.1	4022

2319 model spring is analysed by static & transient method and total deformation under 176.22 mm displacement is shown in Figure 4.14.

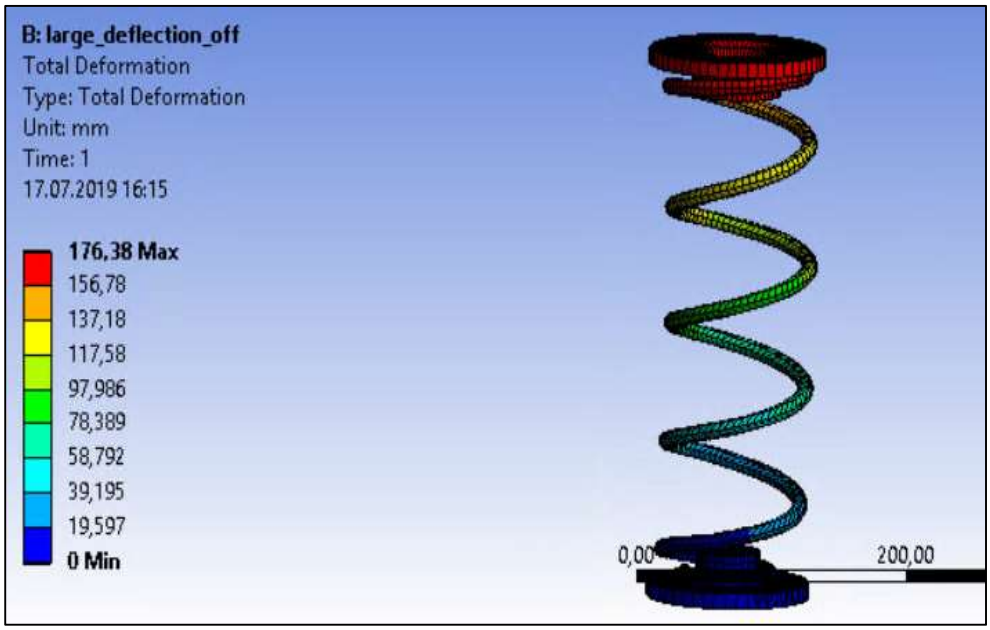

Figure 4.14: Total deformation of 2319 model spring under 176.22 mm displacement, Ansys (Static & Transient) analysis.

2319 model spring is analysed by LS-DYNA method and total deformation under 176.22 mm displacement is shown in Figure 4.15.

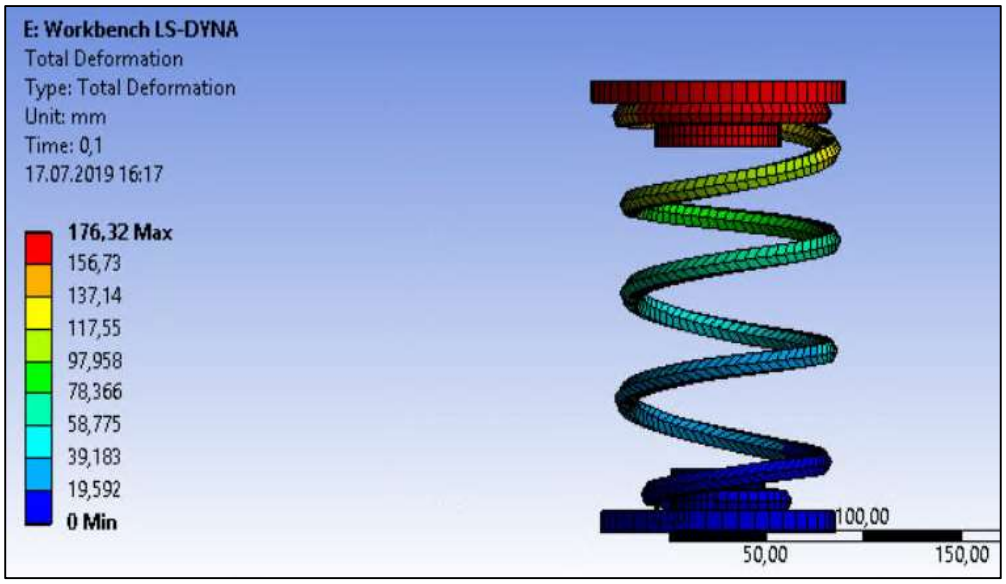

Figure 4.15: Total deformation of 2319 model spring under 176.22 mm displacement, LS-DYNA analysis.

4.2.2. Analysis of 2299A Model Spring

For 2299A model spring the element size, element number and node number are shown in Table 4.12.

Table 4.12: The element size, element number and node number of 2299A model spring.

Element Size (mm)	Element Number	Node Number
5	2819	12152

2299A model spring mesh view is shown in Figure 4.16.

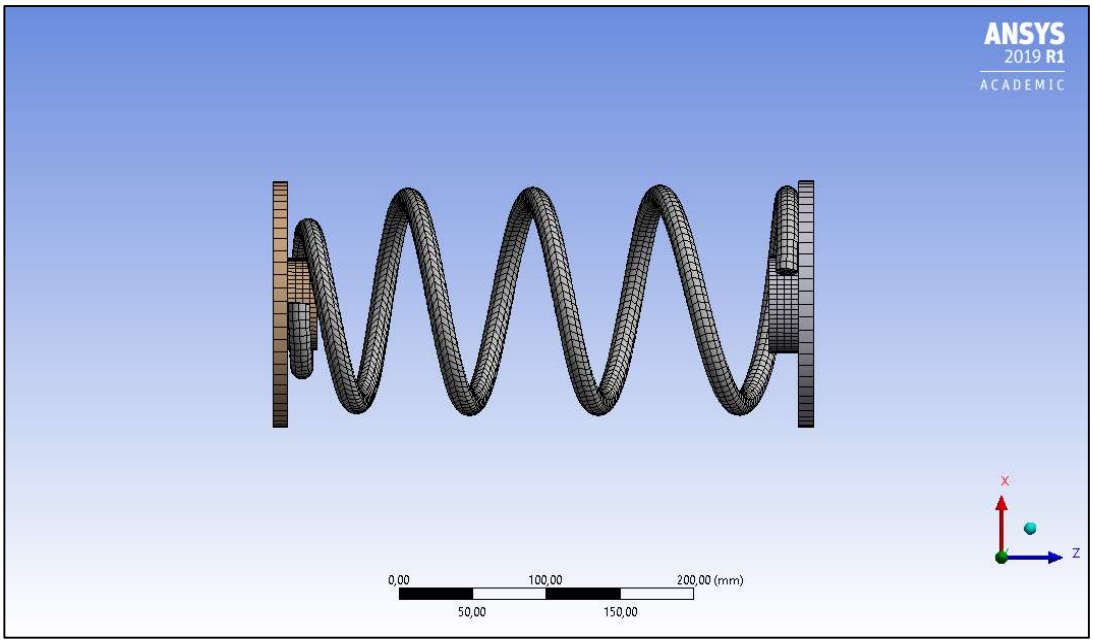

Figure 4.16: Mesh view of 2299A model spring.

Three different cases are analysed. For static structural analyse, boundary conditions that are applied on upper and lower plates are shown in the Table 4.13.

Table 4.13: Boundary conditions for static structual analyse of 2299A model spring.

Cases	Lower plate	Upper plate
Case 1	Fixed Support	Displacement, -z, 76.7 mm
Case 2	Fixed Support	Displacement, -z, 101.7 mm
Case 3	Fixed Support	Displacement, -z, 126.7 mm

For transient structural analyse, boundary conditions that are applied on upper and lower plates are shown in the Table 4.14.

Table 4.14: Boundary conditions for transient structual analyse of 2299A model spring.

Cases	Lower plate	Upper plate	Step End Time
Case 1	Fixed Support	Velocity, -z, 10 mm/s	7.67 s
Case 2	Fixed Support	Velocity, -z, 10 mm/s	10.17 s
Case 3	Fixed Support	Velocity, -z, 10 mm/s	12.67 s

For workbench LS-DYNA (Explicit) analyse, boundary conditions that are applied on upper and lower plates are shown in the Table 4.15.

Table 4.15: Boundary conditions for LS-DYNA (Explicit) analyse of 2299A model spring.

Cases	Lower plate	Upper plate
Case 1	Rigid Body Constraint, All fixed	Displacement, -z, 76.7 mm
Case 2	Rigid Body Constraint, All fixed	Displacement, -z, 101.7 mm
Case 3	Rigid Body Constraint, All fixed	Displacement, -z, 126.7 mm

The 2299A model spring is analysed and the results for 76.7 mm applied displacement are shown in Table 4.16.

Table 4.16: Comparison of calculated reaction forces for applied displacement 76.7 mm.

Analysis Type	Achieved Displacement (mm)	Reaction Force (N)	Reaction Force (Experimental) (N)
Static(Large Deflection Off)	76.975	2429.8	2257
Static(Large Deflection On)	76.978	2378.5	2257
Transient (Implicit)	76.983	2376.7	2257
LS-DYNA (Explicit)	76.981	2110.8	2257

2299A model spring is analysed by static large def. off method and total deformation under 76.7 mm displacement is shown in Figure 4.17.

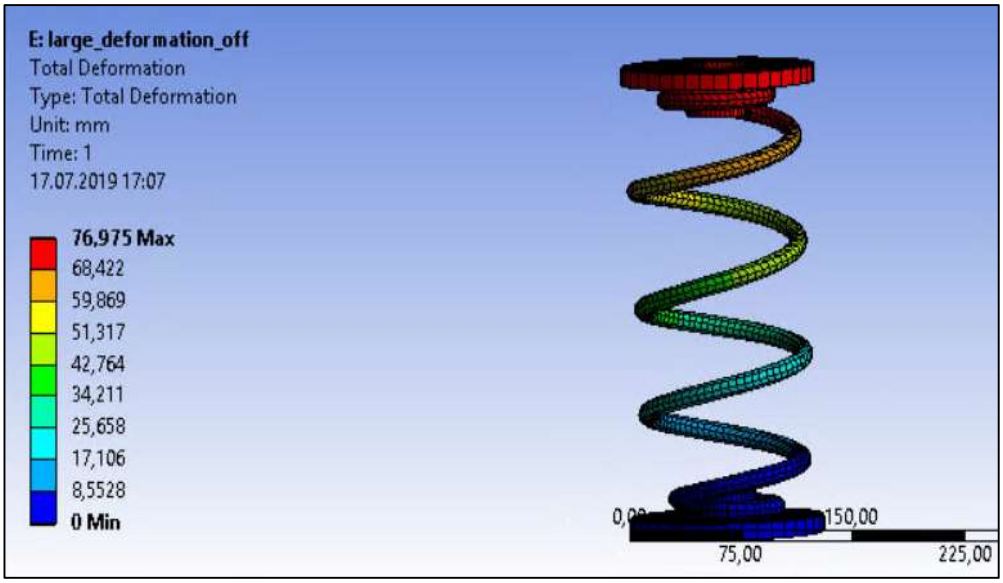

Figure 4.17: Total deformation of 2299A model spring under 76.7 mm displacement, Ansys (Static Large Def. Off) analysis.

2299A model spring is analysed by static large def. on method and total deformation under 76.7 mm displacement is shown in Figure 4.18.

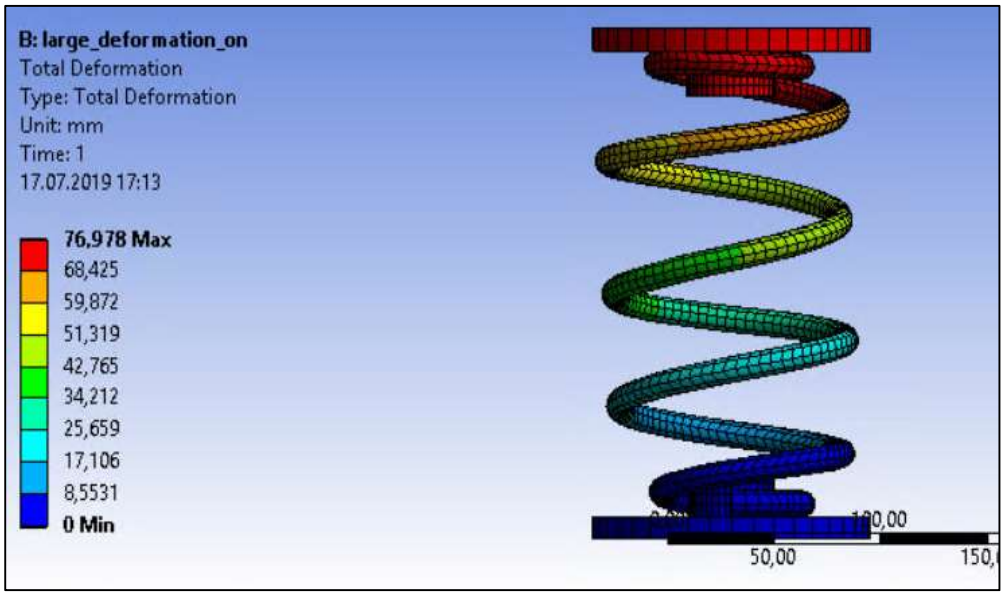

Figure 4.18: Total deformation of 2299A model spring under 76.7 mm displacement, Ansys (Static Large Def. On) analysis.

2299A model spring is analysed by transient structural method and total deformation under 76.7 mm displacement is shown in Figure 4.19.

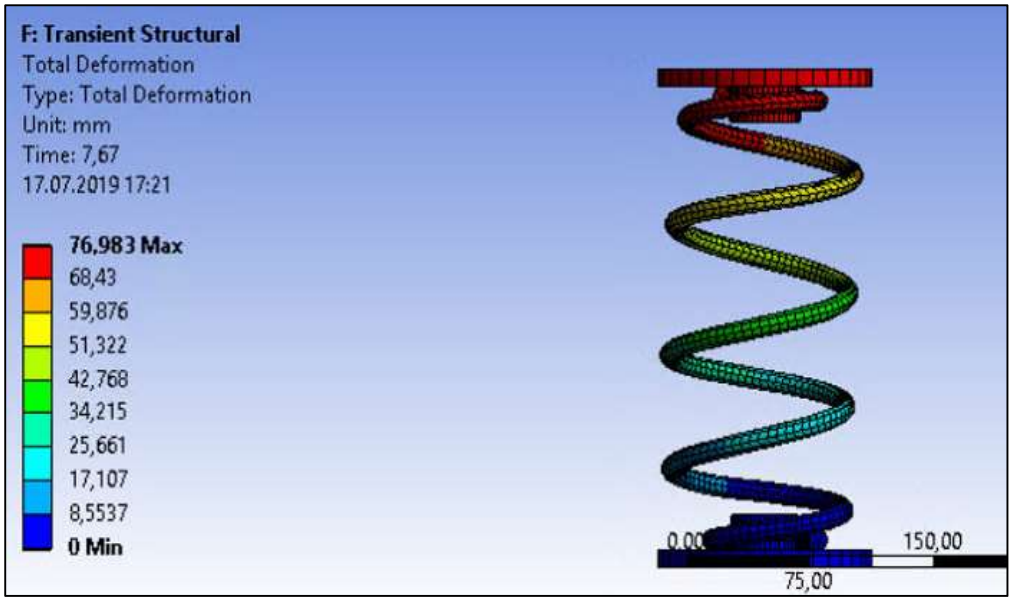

Figure 4.19: Total deformation of 2299A model spring under 76.7 mm displacement, Ansys (Transient Structural) analysis.

2299A model spring is analysed by LS-DYNA method and total deformation under 76.7 mm displacement is shown in Figure 4.20.

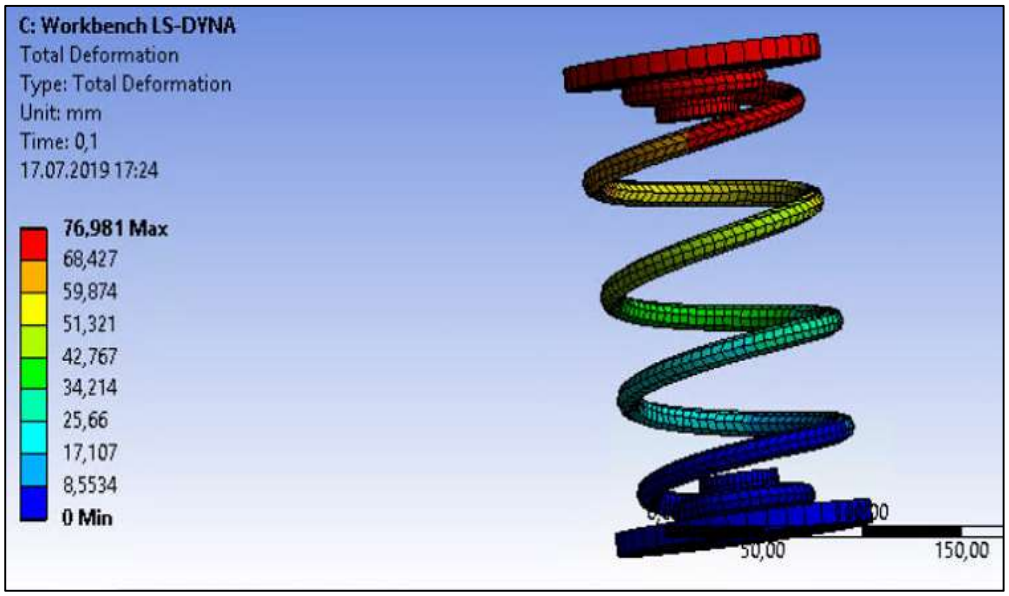

Figure 4.20: Total deformation of 2299A model spring under 76.7 mm displacement, LS-DYNA analysis.

The 2299A model spring is analysed and the results for 101.7 mm applied displacement are shown in Table 4.17.

Table 4.17: Comparison of calculated reaction forces for applied displacement 101.7 mm.

Analysis Type	Achieved Displacement (mm)	Reaction Force (N)	Reaction Force (Experimental) (N)
Static(Large Deflection Off)	102.06	3220.1	2968
Static(Large Deflection On)	102.07	3118.4	2968
Transient (Implicit)	102.08	3133.2	2968
LS-DYNA (Explicit)	101.95	2804.4	2968

2299A model spring is analysed by static large def. off method and total deformation under 101.7 mm displacement is shown in Figure 4.21.

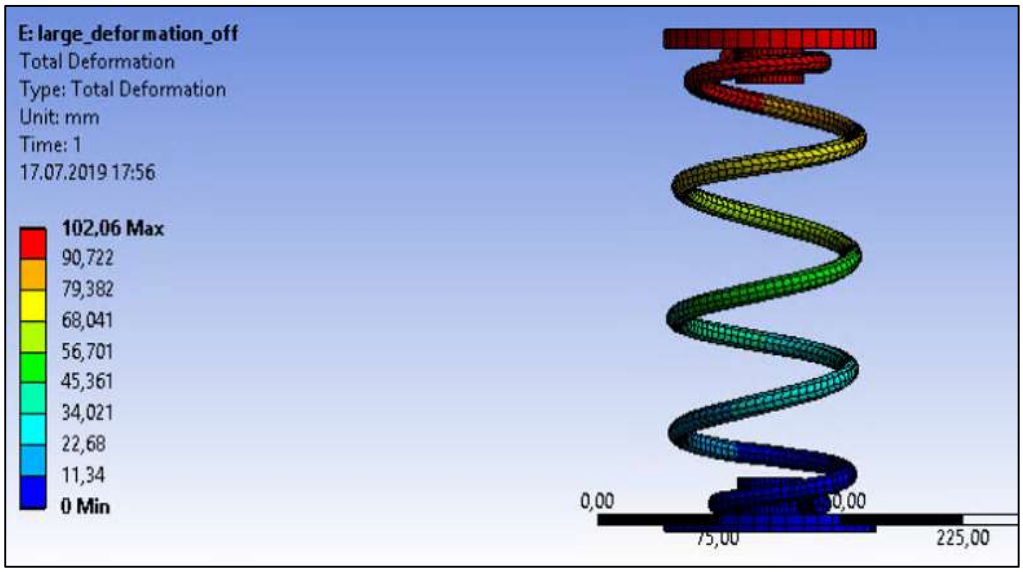

Figure 4.21: Total deformation of 2299A model spring under 101.7 mm displacement, Ansys (Static Large Def. Off) analysis.

2299A model spring is analysed by static large def. on method and total deformation under 101.7 mm displacement is shown in Figure 4.22.

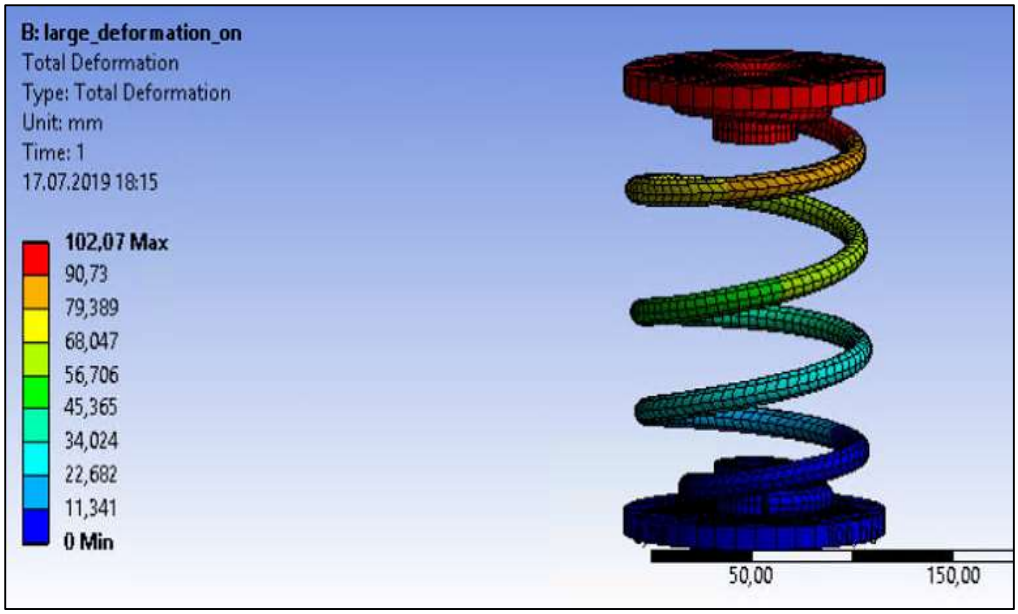

Figure 4.22: Total deformation of 2299A model spring under 101.7 mm displacement, Ansys (Static Large Def. On) analysis.

2299A model spring is analysed by transient structural method and total deformation under 101.7 mm displacement is shown in Figure 4.23.

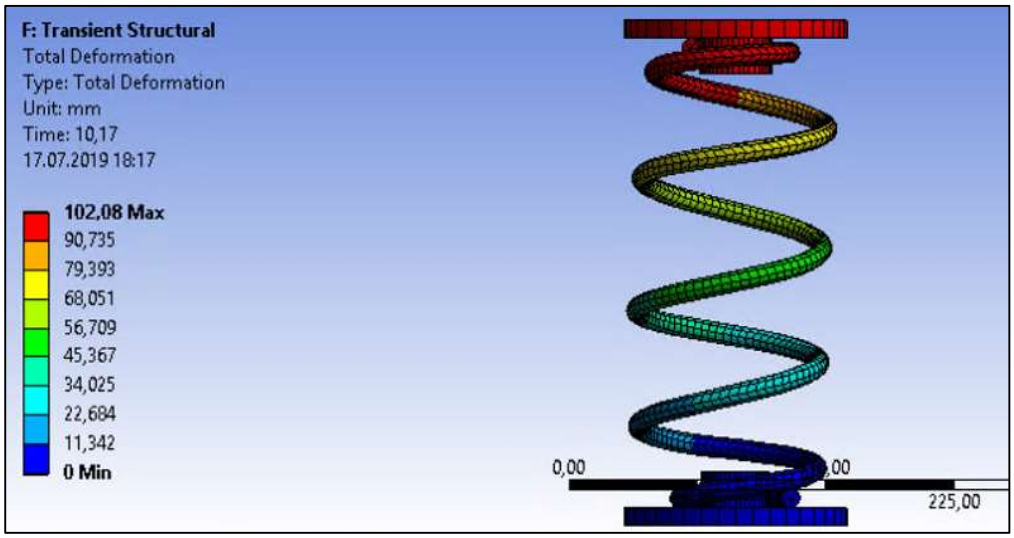

Figure 4.23: Total deformation of 2299A model spring under 101.7 mm displacement, Ansys (Transient Structural) analysis.

2299A model spring is analysed by LS-DYNA method and total deformation under 101.7 mm displacement is shown in Figure 4.24.

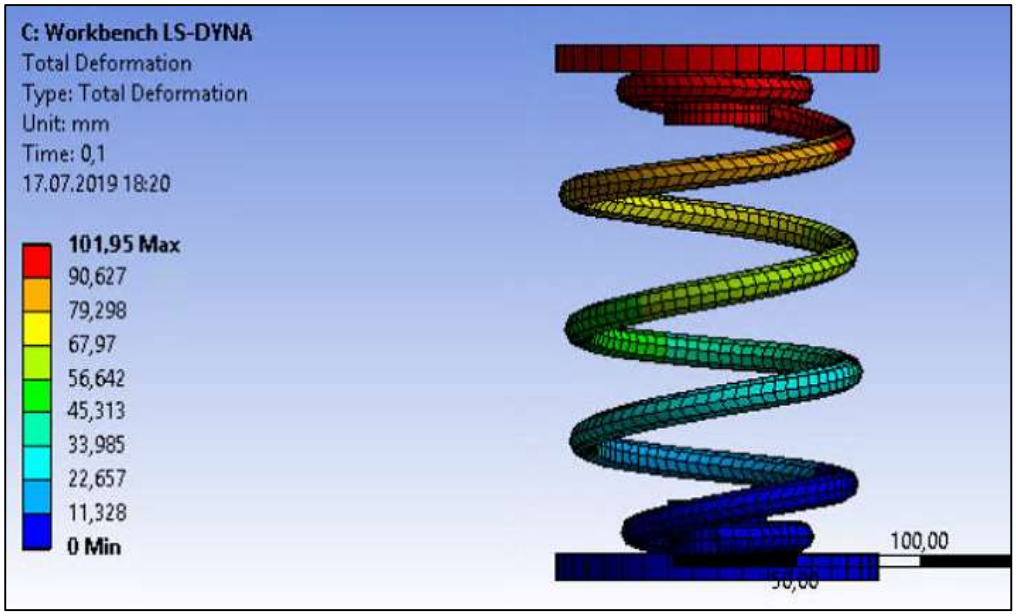

Figure 4.24: Total deformation of 2299A model spring under 101.7 mm displacement, LS-DYNA analysis.

The 2299A model spring is analysed and the results for 126.7 mm applied displacement are shown in Table 4.18.

Table 4.18: Comparison of calculated reaction forces for applied displacement 126.7 mm.

Analysis Type	Achieved Displacement (mm)	Reaction Force (N)	Reaction Force (Experimental) (N)
Static(Large Deflection Off)	127.16	4015.9	3676
Static(Large Deflection On)	127.18	3884.5	3676
Transient (Implicit)	127.18	3879.3	3676
LS-DYNA (Explicit)	126.95	3531.1	3676

2299A model spring is analysed by static large def. off method and total deformation under 126.7 mm displacement is shown in Figure 4.25.

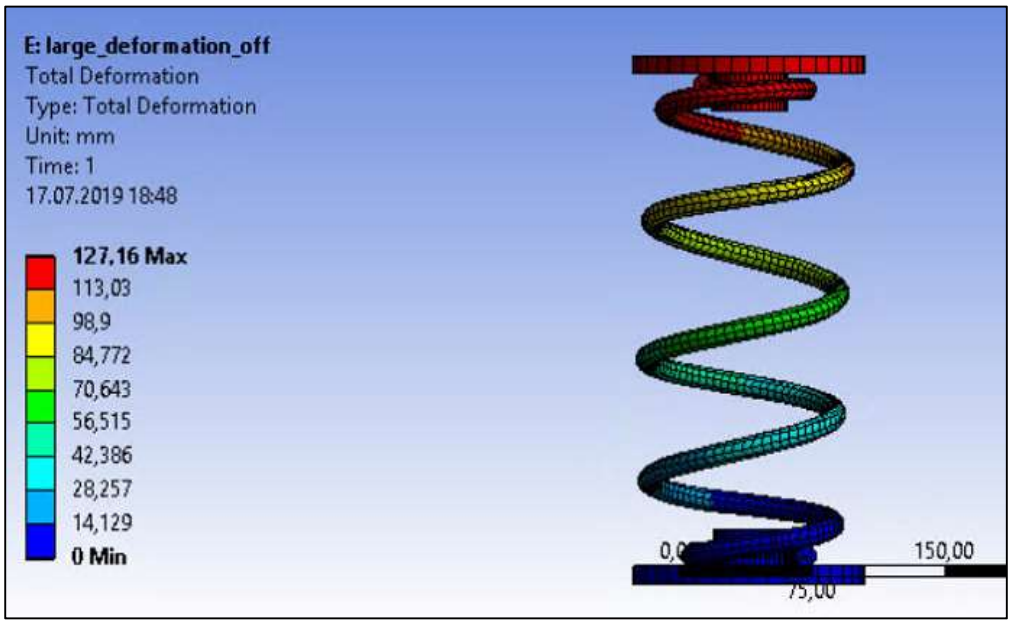

Figure 4.25: Total deformation of 2299A model spring under 126.7 mm displacement, Ansys (Static Large Def. Off) analysis.

2299A model spring is analysed by static large def. on method and total deformation under 126.7 mm displacement is shown in Figure 4.26.

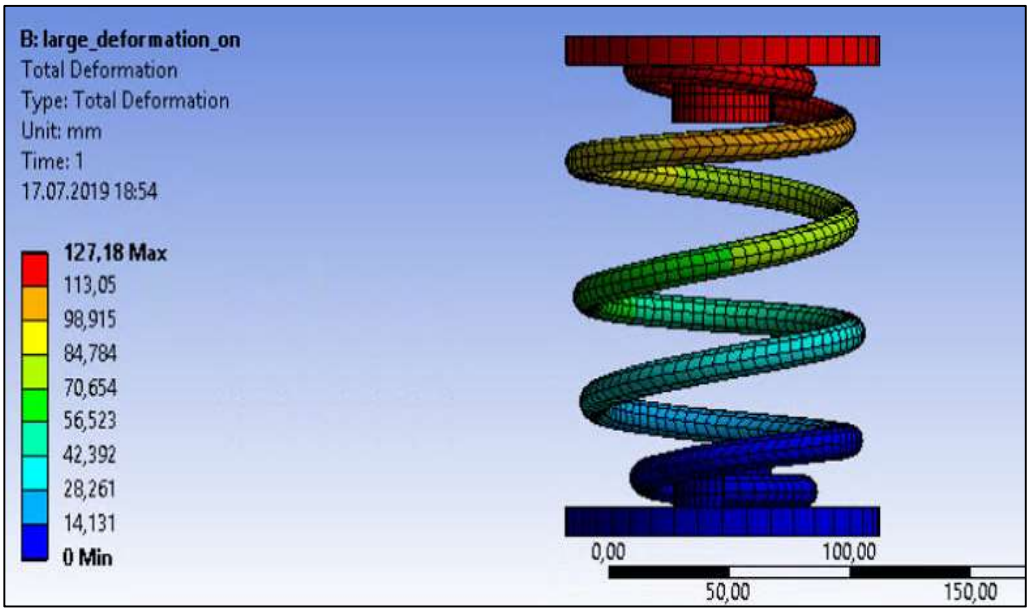

Figure 4.26: Total deformation of 2299A model spring under 126.7 mm displacement, Ansys (Static Large Def. On) analysis.

2299A model spring is analysed by transient structural method and total deformation under 126.7 mm displacement is shown in Figure 4.27.

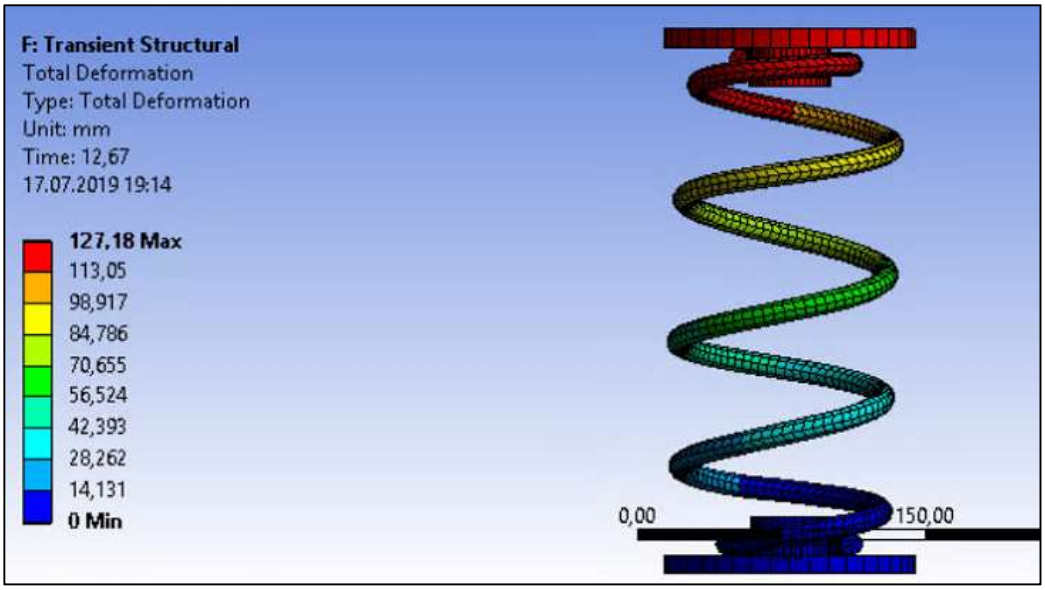

Figure 4.27: Total deformation of 2299A model spring under 126.7 mm displacement, Ansys (Transient Structural) analysis.

2299A model spring is analysed by LS-DYNA method and total deformation under 126.7 mm displacement is shown in Figure 4.28.

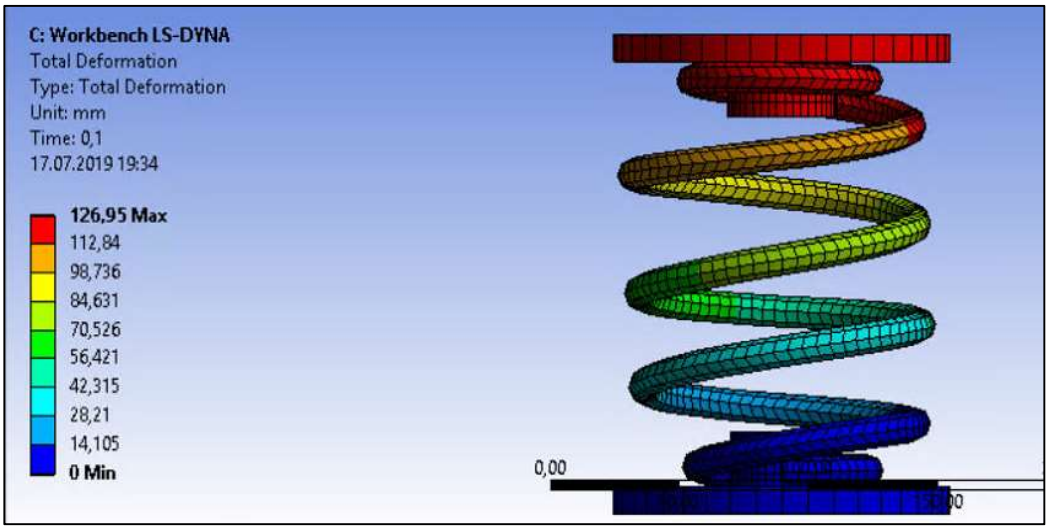

Figure 4.28: Total deformation of 2299A model spring under 126.7 mm displacement, LS-DYNA analysis.

4.2.3. Analysis of 2309 Model Spring

For 2309 model spring the element size, element number and node number are shown in Table 4.19.

Table 4.19: The element size, element number and node number of 2309 model spring.

Element Size (mm)	Element Number	Node Number
5	4765	19497

2309 model spring mesh view is shown in Figure 4.29.

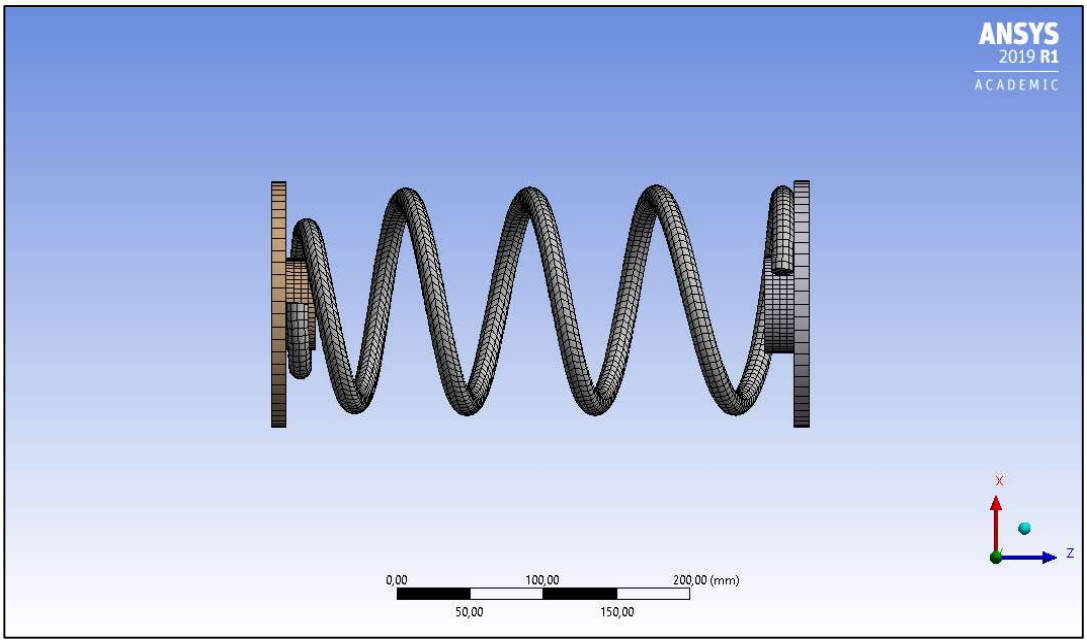

Figure 4.29: Mesh view of 2309 model spring.

Three different cases are analysed. For static structural analysis, boundary conditions that are applied on upper and lower plates are shown in the Table 4.20.

Table 4.20: Boundary conditions for static structual analysis of 2309 model spring.

Cases	Lower plate	Upper plate
Case 1	Fixed Support	Displacement, -z, 71.06 mm
Case 2	Fixed Support	Displacement, -z, 144.06 mm
Case 3	Fixed Support	Displacement, -z, 174.06 mm

For transient structural analysis, boundary conditions that are applied on upper and lower plates are shown in the Table 4.21.

Table 4.21: Boundary conditions for transient structual analysis of 2309 model spring.

Cases	Lower plate	Upper plate	Step End Time
Case 1	Fixed Support	Velocity, -z, 10 mm/s	7.106 s
Case 2	Fixed Support	Velocity, -z, 10 mm/s	14.406 s
Case 3	Fixed Support	Velocity, -z, 10 mm/s	17.406 s

For workbench LS-DYNA (Explicit) analysis, boundary conditions that are applied on upper and lower plates are shown in the Table 4.22

Table 4.22: Boundary conditions for LS-DYNA (Explicit) analysis of 2309 model spring.

Cases	Lower plate	Upper plate
Case 1	Rigid Body Constraint, All fixed	Displacement, -z, 71.06 mm
Case 2	Rigid Body Constraint, All fixed	Displacement, -z, 144.06 mm
Case 3	Rigid Body Constraint, All fixed	Displacement, -z, 174.06 mm

The 2309 model spring is analysed and the results for 71.06 mm applied displacement are shown in Table 4.23.

Table 4.23: Comparison of calculated reaction forces for applied displacement 71.06 mm.

Analysis Type	Achieved Displacement (mm)	Reaction Force (N)	Reaction Force (Experimental) (N)
Static(Large Deflection Off)	71.135	1364.4	1621
Static(Large Deflection On)	71.135	1366.6	1621
Transient (Implicit)	71.135	1351.3	1621
LS-DYNA (Explicit)	72.703	1519.6	1621

2309 model spring is analysed by static large def. off, on & transient method and total deformation under 71.06 mm displacement is shown in Figure 4.30.

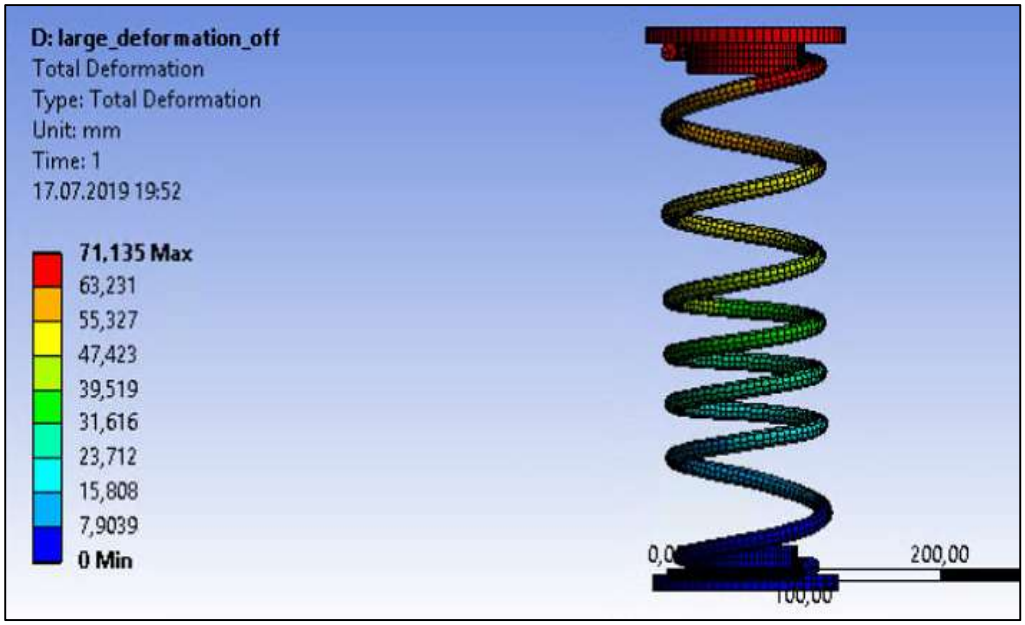

Figure 4.30: Total deformation of 2309 model spring under 71.06 mm displacement, Ansys (Static Large Def. Off & On, Transient) analysis.

2309 model spring is analysed by LS-DYNA method and total deformation under 71.06 mm displacement is shown in Figure 4.31.

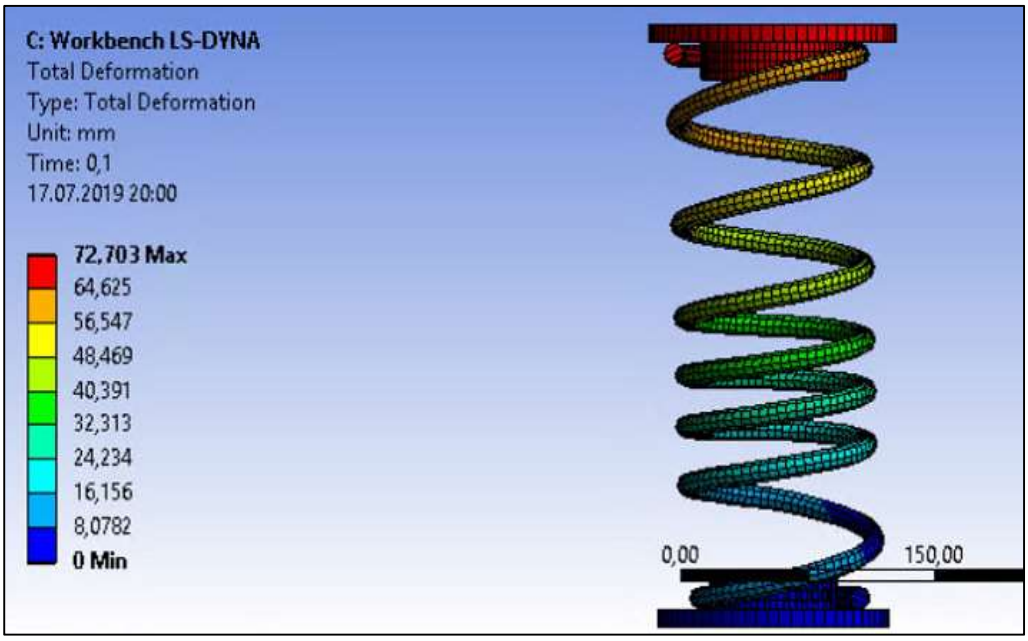

Figure 4.31: Total deformation of 2309 model spring under 71.06 mm displacement, LS-DYNA analysis.

The 2309 model spring is analysed and the results for 144.06 mm applied displacement are shown in Table 4.24.

Table 4.24: Comparison of calculated reaction forces for applied displacement 144.06 mm.

Analysis Type	Achieved Displacement (mm)	Reaction Force (N)	Reaction Force (Experimental) (N)
Static(Large Deflection Off)	144.17	2871.5	3109
Static(Large Deflection On)	144.2	2808.4	3109
Transient (Implicit)	144.21	2801.3	3109
LS-DYNA (Explicit)	145.87	2998.2	3109

2309 model spring is analysed by static large def. off method and total deformation under 144.06 mm displacement is shown in Figure 4.32.

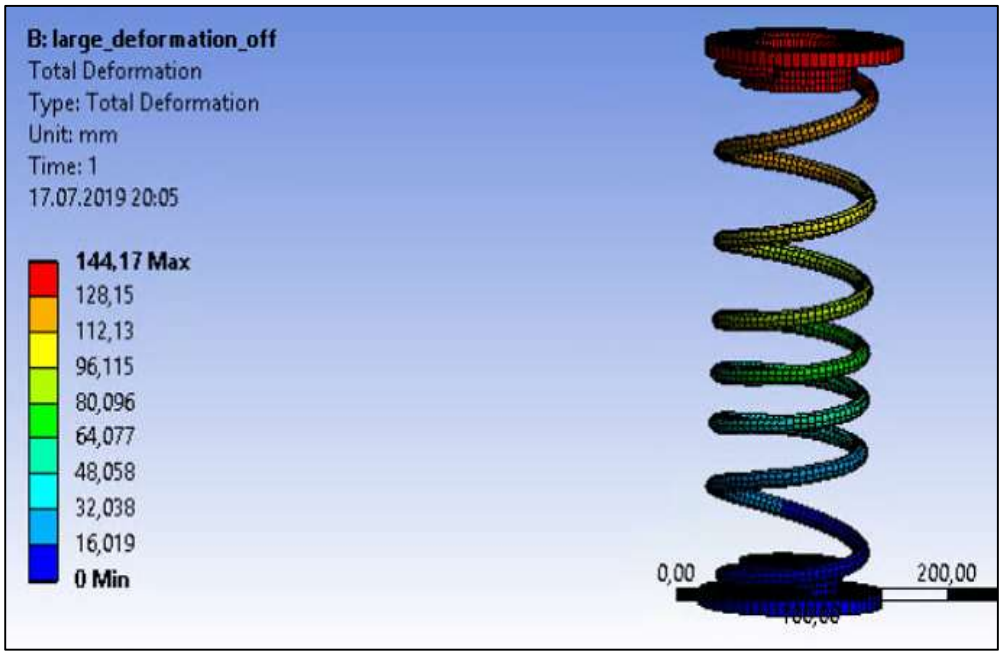

Figure 4.32: Total deformation of 2309 model spring under 144.06 mm displacement, Ansys (Static Large Def. Off) analysis.

2309 model spring is analysed by static large def. on method and total deformation under 144.06 mm displacement is shown in Figure 4.33.

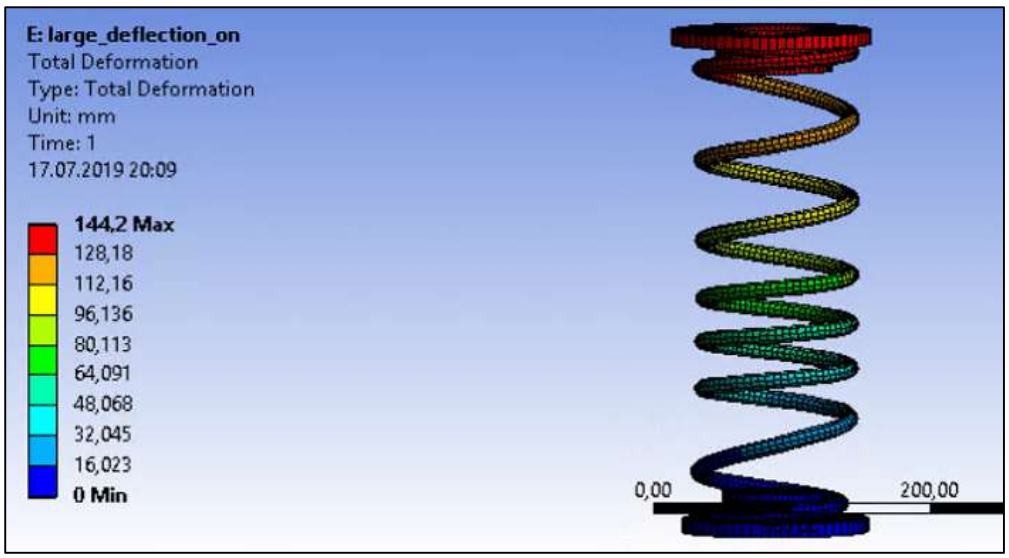

Figure 4.33: Total deformation of 2309 model spring under 144.06 mm displacement, Ansys (Static Large Def. On) analysis.

2309 model spring is analysed by transient structural method and total deformation under 144.06 mm displacement is shown in Figure 4.34.

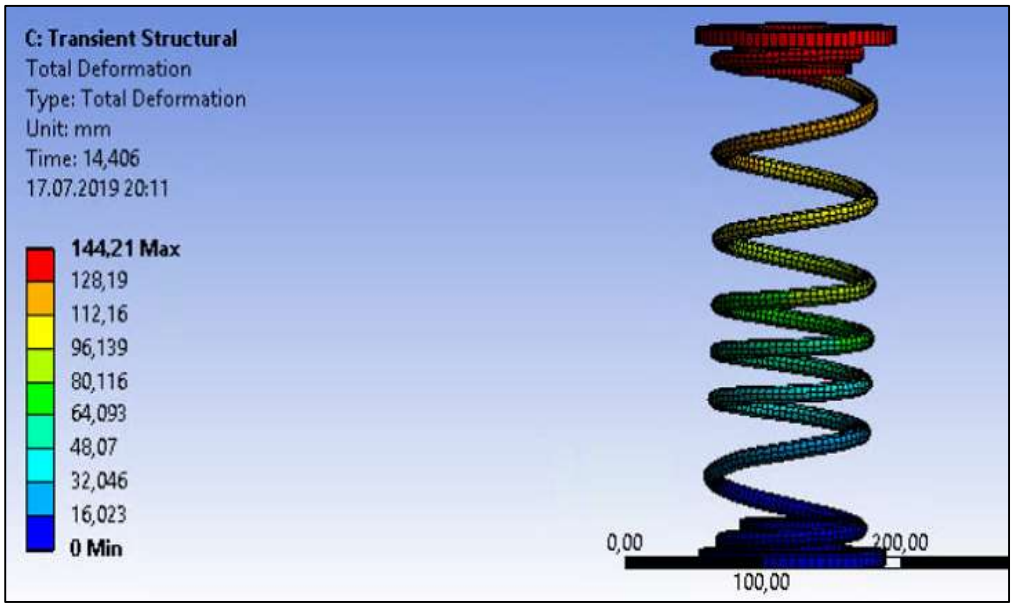

Figure 4.34: Total deformation of 2309 model spring under 144.06 mm displacement, Ansys (Transient Structural) analysis.

2309 model spring is analysed by LS-DYNA method and total deformation under 144.06 mm displacement is shown in Figure 4.35.

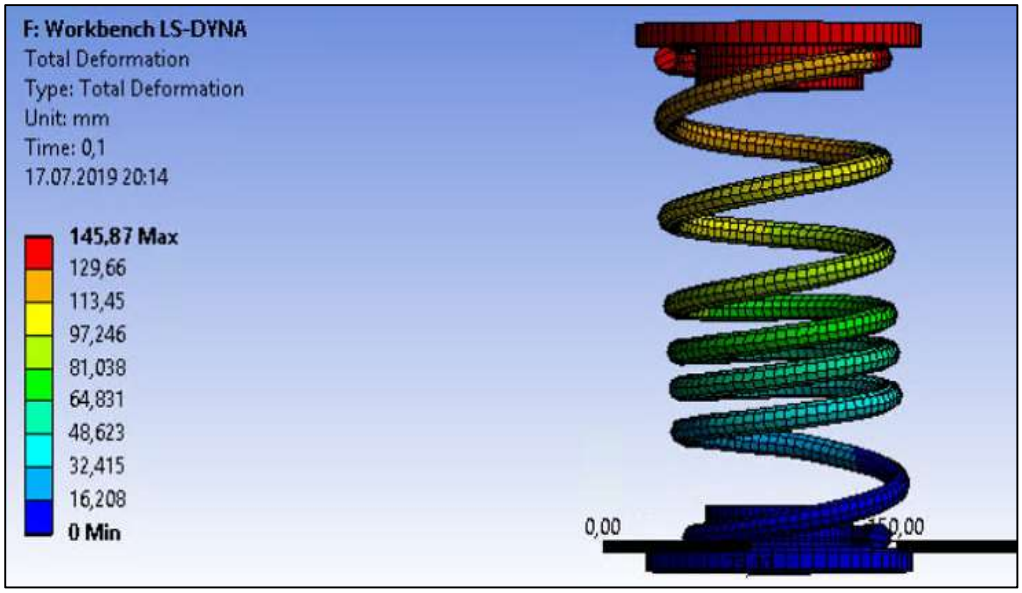

Figure 4.35: Total deformation of 2309 model spring under 144.06 mm displacement, LS-DYNA analysis.

The 2309 model spring is analysed and the results for 174.06 mm applied displacement are shown in Table 4.25.

Table 4.25: Comparison of calculated reaction forces for applied displacement 174.06 mm.

Analysis Type	Achieved Displacement (mm)	Reaction Force (N)	Reaction Force (Experimental) (N)
Static(Large Deflection Off)	174.2	3469.5	3774
Static(Large Deflection On)	174.23	3385.9	3774
Transient (Implicit)	174.24	3376.4	3774
LS-DYNA (Explicit)	175.64	3686.7	3774

2309 model spring is analysed by static large def. off method and total deformation under 174.06 mm displacement is shown in Figure 4.36.

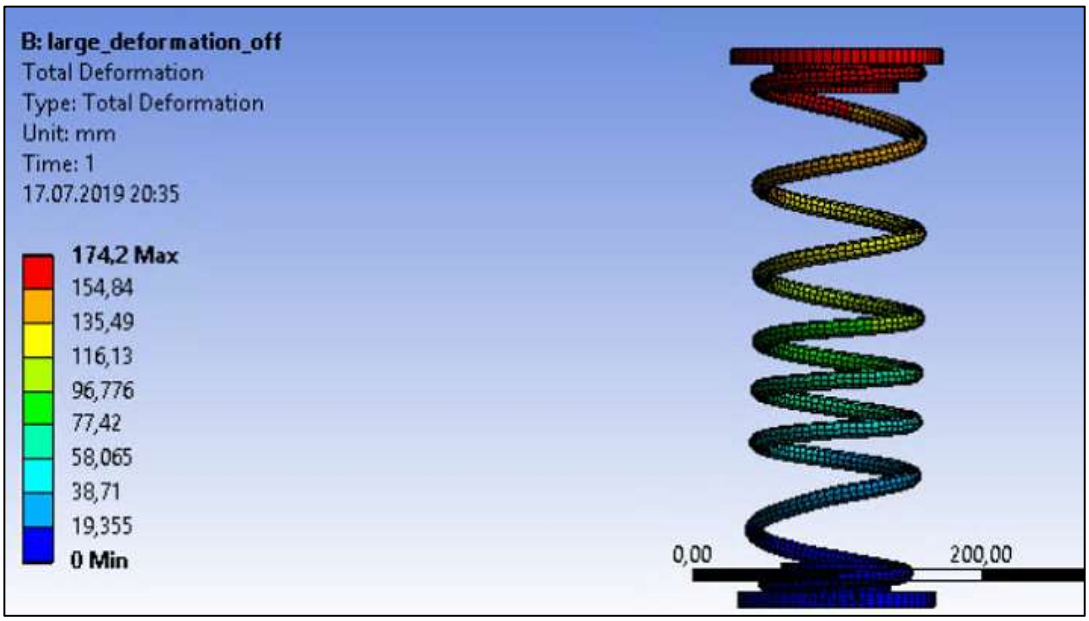

Figure 4.36: Total deformation of 2309 model spring under 174.06 mm displacement, Ansys (Static Large Def. Off) analysis.

2309 model spring is analysed by static large def. on method and total deformation under 174.06 mm displacement is shown in Figure 4.37.

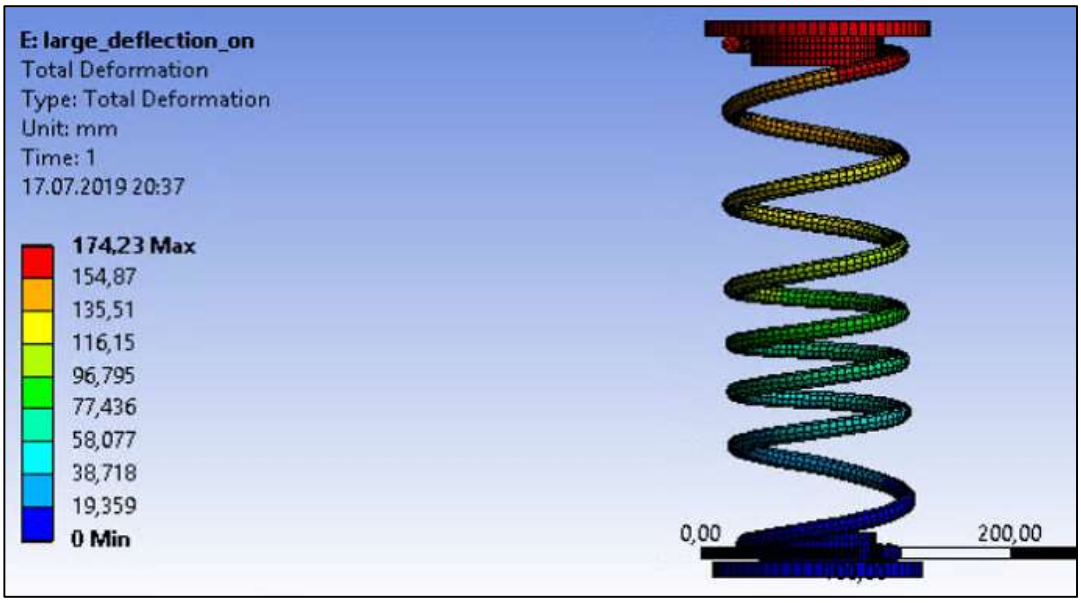

Figure 4.37: Total deformation of 2309 model spring under 174.06 mm displacement, Ansys (Static Large Def. On) analysis.

2309 model spring is analysed by transient structural method and total deformation under 174.06 mm displacement is shown in Figure 4.38.

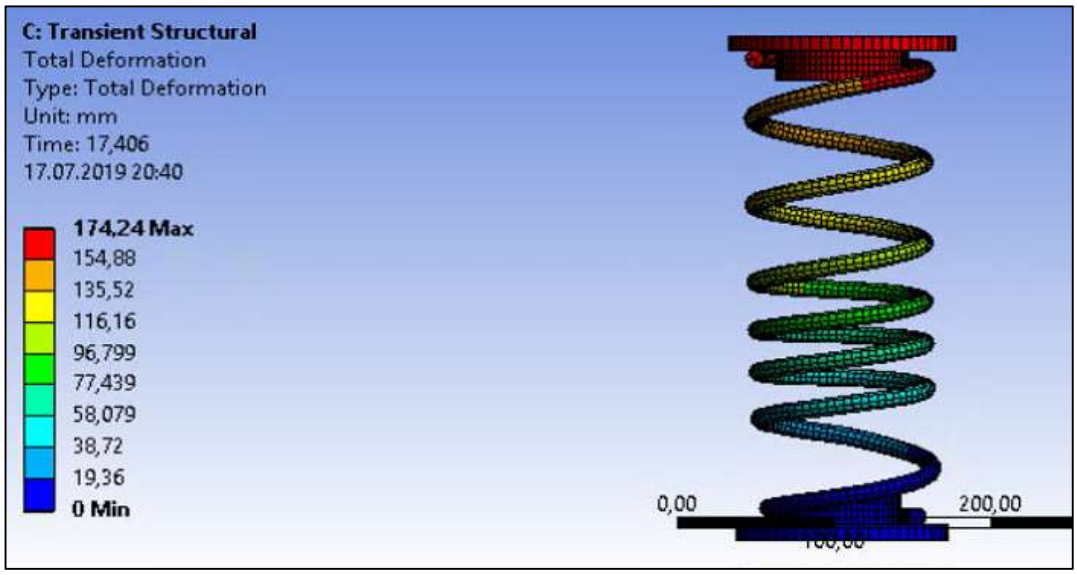

Figure 4.38: Total deformation of 2309 model spring under 174.06 mm displacement, Ansys (Transient Structural) analysis.

2309 model spring is analysed by LS-DYNA method and total deformation under 174.06 mm displacement is shown in Figure 4.39.

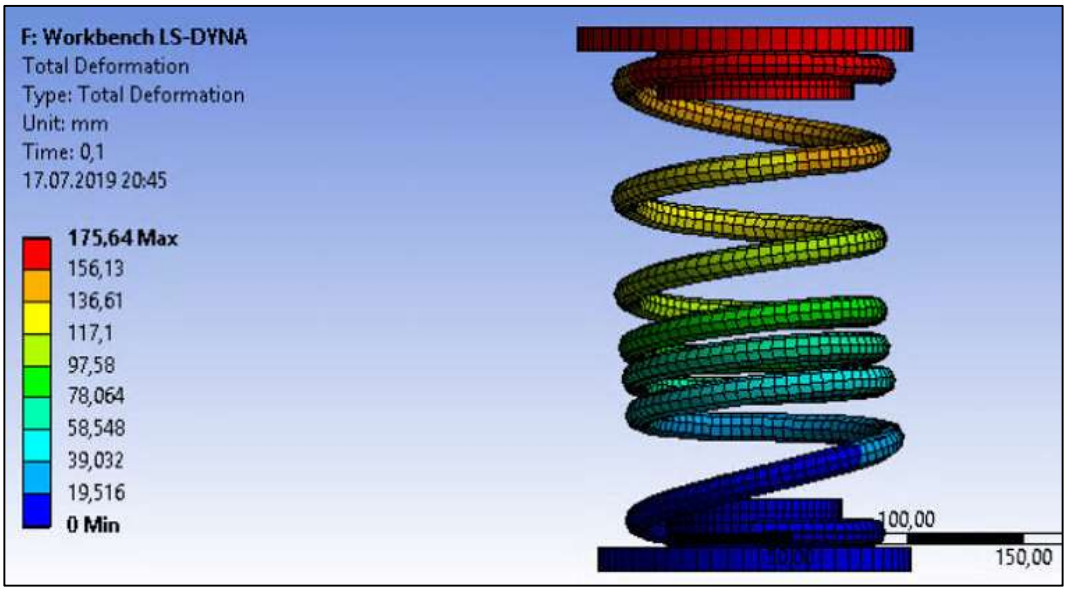

Figure 4.39: Total deformation of 2309 model spring under 174.06 mm displacement, LS-DYNA analysis.

4.2.4. Analysis of 2304A Model Spring

For 2304A model spring the element size, element number and node number are shown in Table 4.26.

Table 4.26: The element size, element number and node number of 2304A model spring.

Element Size (mm)	Element Number	Node Number
5	25207	21155

2304A model spring mesh view is shown in Figure 4.40.

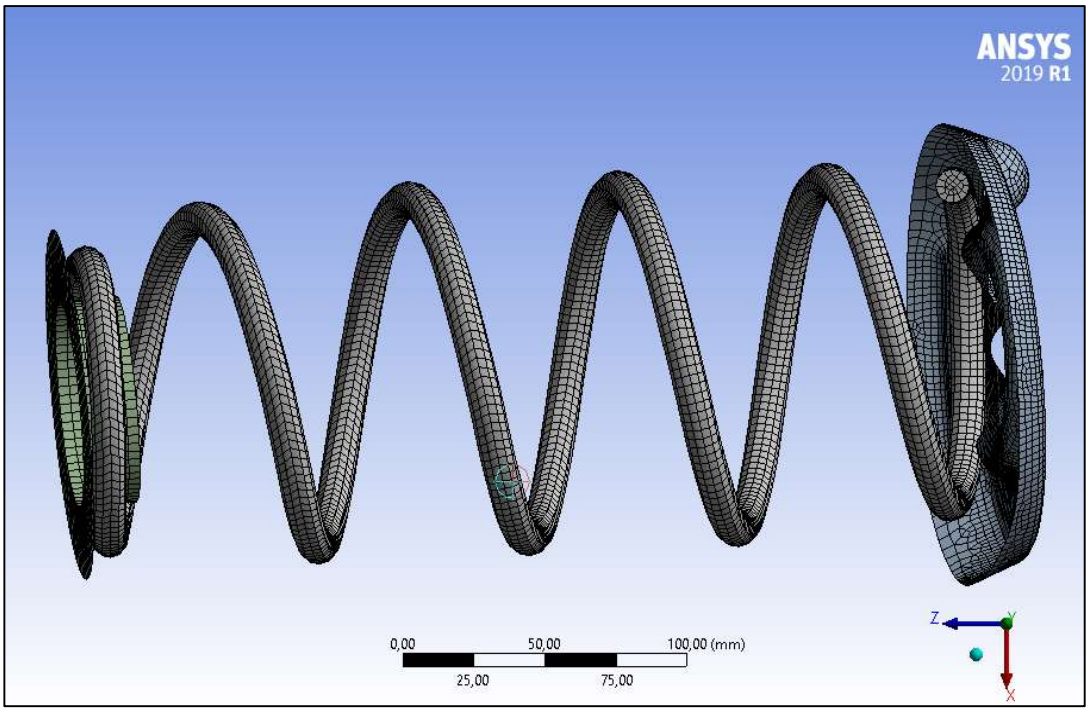

Figure 4.40: Mesh view of 2304A model spring.

2304A model spring parts' mesh types are shown in Figure 4.41.

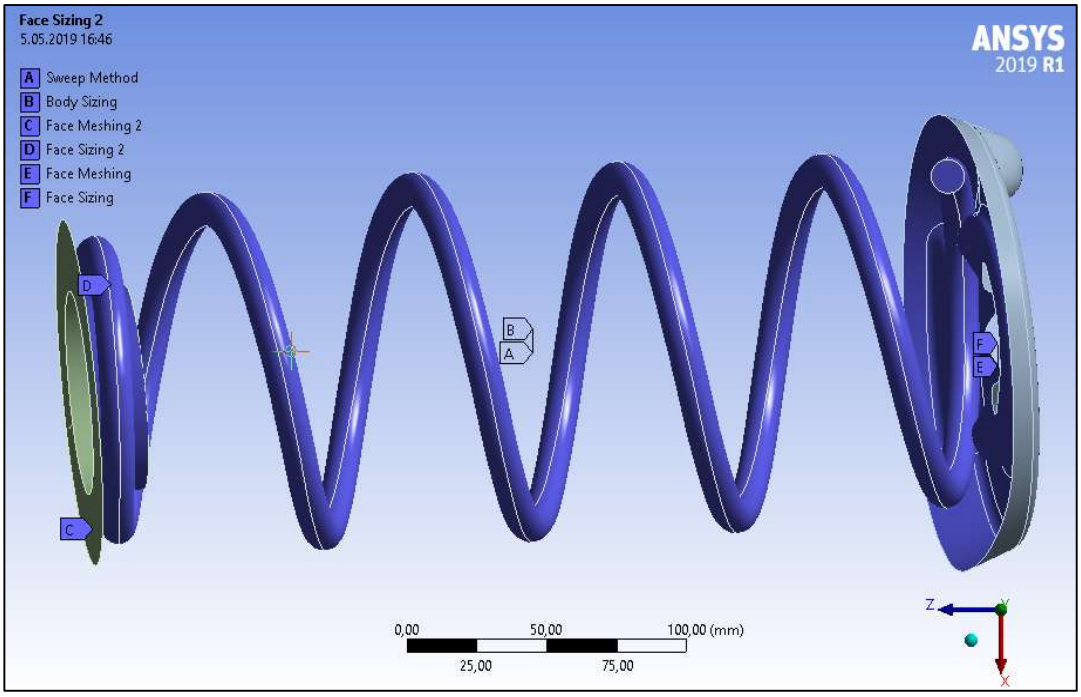

Figure 4.41: Mesh of 2304A model spring parts.

2304A is analysed by LS-DYNA (Explicit) method only. Static structural and transient analysis can not analyse because the displacement which is applied causes large deformation. Just one case is applied and shown in the Table 4.27.

Table 4.27: Boundary conditions for LS-DYNA (Explicit) analysis of 2304A model spring.

Cases	Lower plate	Upper plate
Case 1	Fixed Support	Remote Displacement, -z, 181 mm

Analysis settings are shown in Figure 4.42.

Details of "Analysis Settings"	
Step Controls	
End Time	0,1
Time Step Safety Factor	0,9
Maximum Number Of Cycles	10000000
Automatic Mass Scaling	Yes
Time Step Size	1E-07
CPU and Memory Management	
Memory Allocation	Program Controlled
Number Of CPUS	1
Processing Type	Program Controlled
Solver Controls	
Solver Type	Program Controlled
Solver Precision	Program Controlled
Unit System	nmm
Initial Velocities	
Initial Velocities are applied immediately	Yes
Damping Controls	
Global Damping	No
Hourglass Controls	
ALE Controls	
Joint Controls	
Composite Controls	
Output Controls	
Time History Output Controls	
Analysis Data Management	

Figure 4.42: Analysis settings of 2304A model spring.

The 2304A model spring's force line is not straight so total reaction force is resultant force of reaction force in z and y direction. Reaction force in y direction is

lateral force. The applied force is in z direction but reaction forces are vertical and lateral. Results for 181 mm applied displacement are shown in Table 4.28.

Table 4.28: Comparison of calculated reaction forces for applied displacement 181 mm.

Analysis Type	Achieved Displacement (mm)	Reaction Force (N) Z direction	Reaction Force (N) Y direction	Resultant Force (N)	Reaction Force (Experimental) (N)
LS-DYNA (Explicit)	181.7	3993.1	873.4	4087.5	4305

2304A model spring is analysed by LS-DYNA method and total deformation under 181 mm displacement is shown in Figure 4.43.

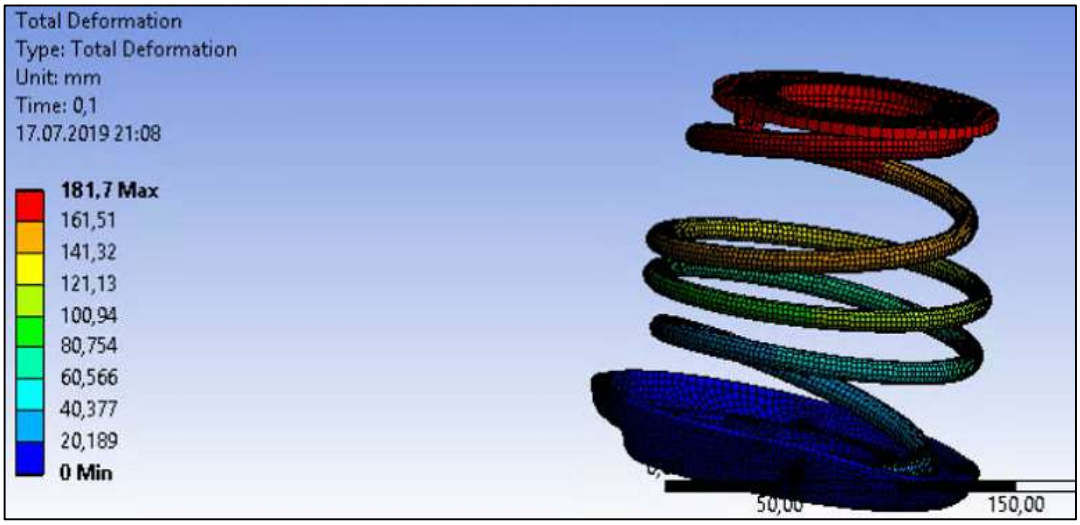

Figure 4.43: Total deformation of 2304A model spring under 181 mm displacement, LS-DYNA analysis.

4.3. Analysis of Spring Models by LS-DYNA

Different analysis types are applied to spring models and it is seen that the results, got from the Ls-Dyna, are the nearest values to the test results. However, for some spring models and boundary conditions the difference between test and analysis results are bigger than 1,5%. To get closer results, some values in the “Analysis

Settings" are changed and mesh sizing is made smaller. Mesh element size is 2,5 mm and "Analysis settings" is shown in Figure 4.44.

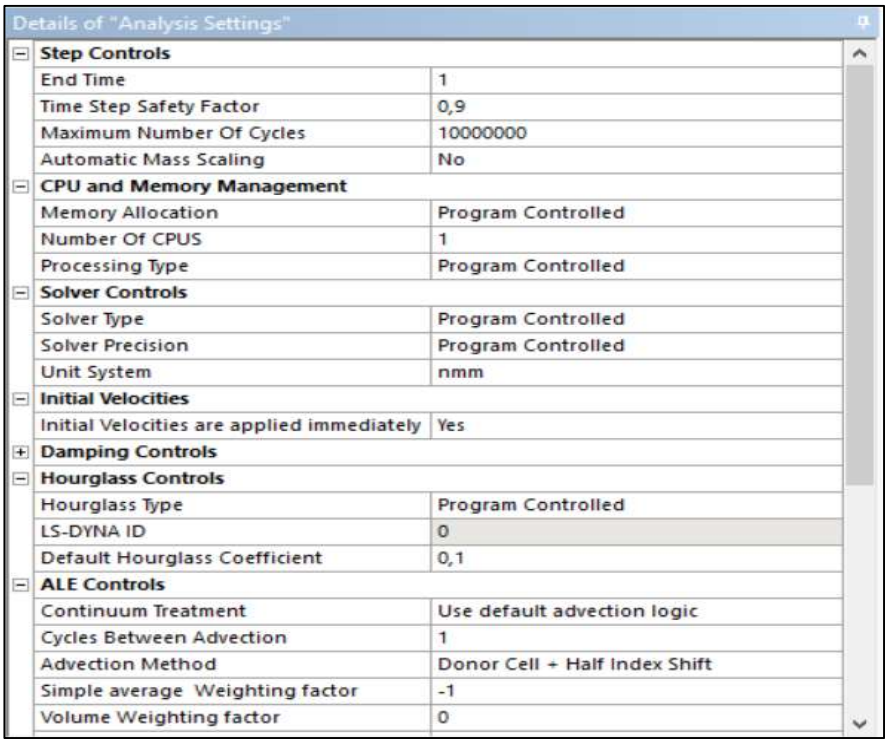

Details of "Analysis Settings"	
Step Controls	
End Time	1
Time Step Safety Factor	0,9
Maximum Number Of Cycles	10000000
Automatic Mass Scaling	No
CPU and Memory Management	
Memory Allocation	Program Controlled
Number Of CPUS	1
Processing Type	Program Controlled
Solver Controls	
Solver Type	Program Controlled
Solver Precision	Program Controlled
Unit System	nmm
Initial Velocities	
Initial Velocities are applied immediately	Yes
Damping Controls	
Hourglass Controls	
Hourglass Type	Program Controlled
LS-DYNA ID	0
Default Hourglass Coefficient	0,1
ALE Controls	
Continuum Treatment	Use default advection logic
Cycles Between Advection	1
Advection Method	Donor Cell + Half Index Shift
Simple average Weighting factor	-1
Volume Weighting factor	0

Figure 4.44: Analysis Settings in LS-DYNA analysis.

Each spring model is analysed with the same analysis settings and mesh sizing. Boundary conditions for each spring model are shown in Table 4.29 and analysis results for each spring model are shown in Table 4.30.

Table 4.29: Boundary conditions for each spring model.

Spring Models	Lower plate	Upper plate
2304A	Rigid Body Constraint, Fixed	Displacement, -z, 181 mm
2319	Rigid Body Constraint, Fixed	Displacement, -z, 176.22 mm
2299A	Rigid Body Constraint, Fixed	Displacement, -z, 126.7 mm
2309	Rigid Body Constraint, Fixed	Displacement, -z, 174.06 mm

Table 4.30: Results for each spring model.

Spring Models	Analysis Results (N)	Test Results (N)
2299A	3717.6	3676
2319	3976.3	4022
2304A	4087.5	4305
2309	3686.7	3774

4.4. Optimization of 2304A Spring Model

2304A spring's wire diameter is constant along the coil. Different type of springs are modeled by Creo Parametric and their wire diameter is changed along their coils. Same displacement (181 mm) is applied all of them and resultant forces are gotten. The analysis are made by LS-DYNA and results are shown in Table 4.31. Top wire diameter and bottom wire diameter is shown in Figure 4.45.

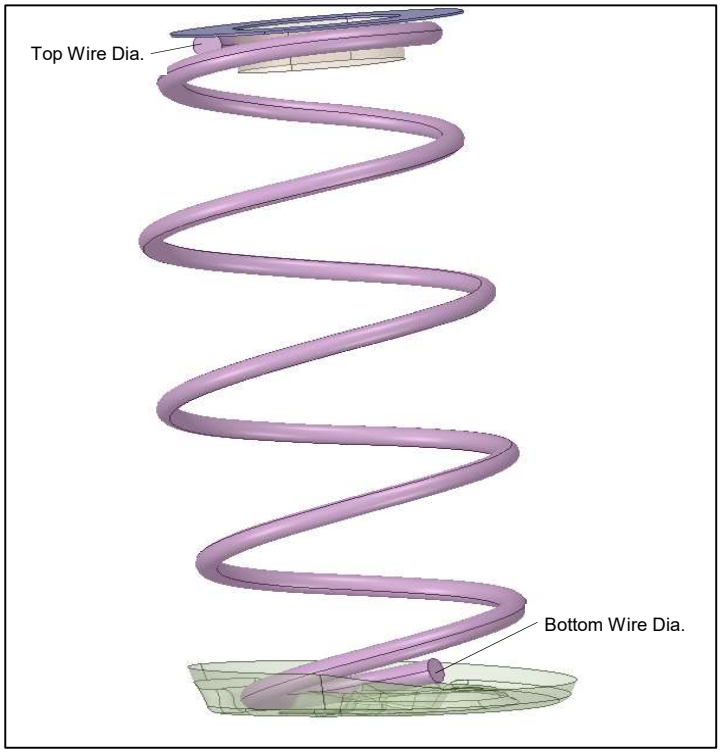

Figure 4.45: 2304A spring model top & bottom wire diameter.

Table 4.31: Results for different wire diameter.

Top wire dia. (mm)	Bottom wire dia. (mm)	Lateral Reac. F. (N)	Vertical Reac. F. (N)	Resultant Force (N)	Mass (kg)
14	9.8	406.0	4243.0	4263.30	1.31
13	10.8	419.8	4390.2	4410.20	1.29
12.5	11.3	287.4	4407.7	4417.06	1.29
11.9	11.9	873.4	3993.1	4087.50	1.29
11.3	12.5	413.7	3312.2	3337.90	1.29
10.8	13	217.0	3245.0	3252.25	1.29
9.8	14	436.5	2614.7	2650.90	1.31

As it is seen from the table, the more top wire diameter increase, the more resultant force increase. However, there is a limit for the optimum spring model. Mass of spring does not change so decrease in mass was not achieved but with the same mass, more resultant force achieved.

5. CONCLUSION

Within this thesis, four car's helical springs are analysed with FEA and the results are compared with test results as Rozmas firm needs. One of these springs' force and spring line was oblique so lateral force is existed. The springs' 3D model and test results have been provided by Rozmas. The results that are obtained listed below.

- Mainly two analysis types are conducted which are implicit and explicit. It has been seen that explicit method is best for large deformed and exposed to self contact springs. Self contact problems can be solved by "Body interaction" specification in LS-DYNA. Figure 5.1 shows a self contact condition.
- Spring models that have straight force line, are analysed by LS-DYNA with 5 mm mesh size and analysis end time was 0.1 s. Within these conditions, it has been seen that the difference between test results are bigger than 1.5%. So, mesh size is decreased to 2.5 mm and analysis end time increased to 1 s. As a result, the difference became smaller than 1.5%.

- 2304A spring model is applied large deformation, so static structural and transient structural analysis could not solve. It is analysed by LS-DYNA and the difference between test result is 5%. This amount of difference is a result of its oblique force and spring line. Also, these lines are not coincident like other spring models.
- An optimization work is conducted for 2304A model spring. Six CAD model is created. Their coil paths are the same with original spring model but wire diameter are different. Moreover, the new CAD models' wire diameters change along the coil. As a result, it has seen that spring with changing wire diameter can absorb bigger amount of force.

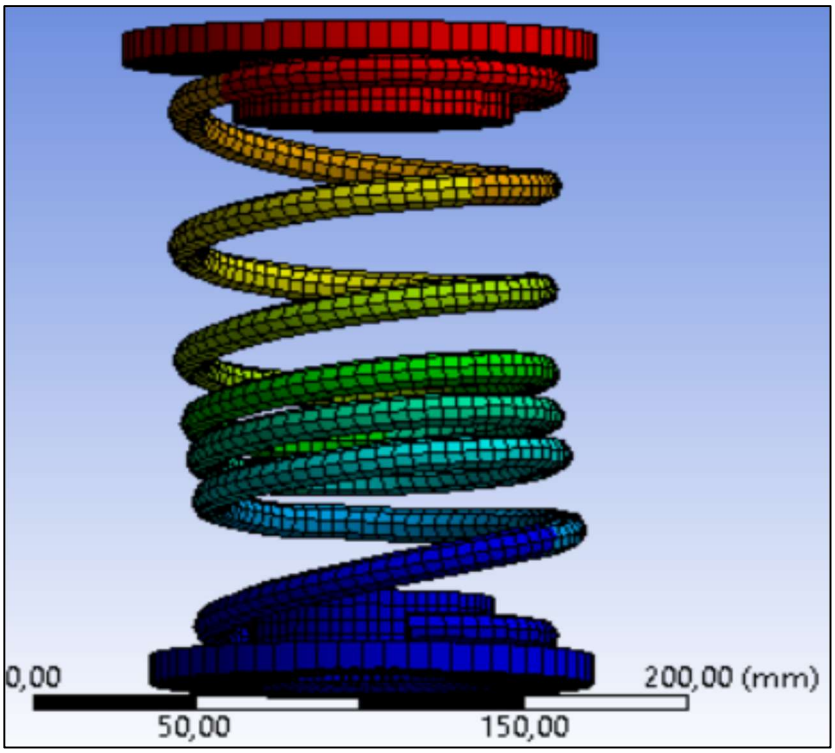

Figure 5.1: Self contact condition.

Static strucural, transient structural (implicit) and LS-DYNA methods are tried for analysis of some pigtail springs. Due to lack of time and resources, the study is limited with 4 spring models. For future works, more spring models can be analysed. Moreover, effect of coil diameter and path can be seen.

REFERENCES

[1] Ameen H. A., Mashloosh M. K., Razooqi I. A., (2014), "Compression and Impact Characterization of Helical and Slotted Cylinder Springs", International Journal of Engineering & Technology, 3 (2), 268-278.

[2] Ansys Theory Reference Release 5.6.

[3] Gundre S. N., Wankhade P. A., (2013), "A Finite Element Analysis of Helical Compression Spring for Electric Tricycle Vehicle Automotive Front Suspension", International Journal of Engineering Research and Technology, 2278-0181.

[4] Kadlag V. L., Thakare P. P., (2017), "Design and Analysis of Helical Compression Spring for Special Purpose Application", International Journal of Advance Research and Innovative Ideas in Education, (0)-2395-4396.

[5] Kaiser B., Berger C., (2006), "Results of Very High Cycle Fatigue Tests on Helical Compression Spring", International Journal of Fatigue, 28 (11), 1658-1663.

[6] Kaoua S. A., Taibi K., Benghanem N., Azouaoui K., Azzaz M. (2011), "Numerical Modelling of Twin Helical Spring Under Tensile Loading", Applied Mathematical Modelling, 35 (3), 1378-1387.

[7] LS-DYNA Theory Manual.

[8] Pinjarla P., Lakshmana Kishore T., (2018), "Design and Analysis of a Shock Absorber", International Journal of Research in Engineering and Technology, 2319-1163.

[9] Pollanen I., Martikka H., (2010), "Optimal re-design of helical Springs Using Fuzzy Design and FEM", Advances in Engineering Software, 41 (3), 410-414.

[10] Prawoto Y., Ikeda M., Manville S. K., Nishikawa A., (2008), "Design and Failure Modes of Automotive Suspension Springs", Engineering Failure Analysis, 15 (8), 1155-1174.

[11] Sameer S., (2015), "Finite Element Analysis of Fatigue Life of Suspension Coil Spring", Master Thesis, Oriental Institute of Science and Technology Bhopal India.

[12] Sequeira A. A., Singh R. K., Shetti G. K., (2016), "Comparative Analysis of Helical Steel Springs with Composite Springs Using Finite Element Method", Journal of Mechanical Engineering and Automation, 6 (5A), 63-70.

[13] Sharma P., Vadodaria D., Jain S. C., (2014), "McPerson Suspension System – A Review", International Journal For Technological Research in Engineering, 1 (12), 2347-4718.

[14] Shijil P., Albin V., Aswin D., Chrisitn J., Josin J., (2016), “Design and Analysis of Suspension System for an All Terrain Vehicle”, International Journal of Scientific & Engineering Research, 7 (3), 2229-5518.

[15] Shpetim L., Stanislov P., Naser L., Afrim G., Jose P., Saso E., (2013), “Design of Independent Suspension Mechanism for a Terrain Vehicle with Four Wheels Drive and Four Wheels Steering", International Journal of Engineering, 11 (1), 1584-2665.

[16] Sonawane P. M., Aher V. K., (2012), “Static and Fatigue Analysis of Multi Leaf Spring Used in The Suspension System of LCV”, International Journal of Engineering Research and Applications, 2 (4), 2248-9622.

[17] Xianfu C., Yugun L., (2014), “Multiobjective Robust Design of the Double Wishbone Suspension System Based on Particle Swarm Optimization”, Scientific World Journal, 2014 (3), 354857.

[18] Yalasangi V. V., Naniwadekar A.M., (2016), “An Overview of Analysis of Torsion Bar of Light Motor Vehicle Car with Nonlinear Parameter”, International Advanced Research Journal in Science, Engineering and Technology, 3 (8), 2393-8021.

[19] Yanli W., Youli Z., Yuanlin H., (2014), “Failure Analysis of a Helical Compression Spring for a Heavy Vehicle’s Suspension System”, Case Studies in Engineering Failure Analysis, 2 (2), 169-173.

[20] Web 1, (2019), https://www.researchgate.net/, (Access Date: 01/01/2019).

[21] Web 2, (2019), https://axleaddict.com/, (Access Date: 05/01/2019).

[22] Web 3, (2019), https:// aa1car.com/, (Access Date: 10/01/2019).

[23] Web 4, (2019), https:// carid.com/, (Access Date: 10/01/2019).

[24] Web 5, (2019), https:// competitionx.com/, (Access Date: 12/01/2019).

[25] Web 6, (2019), https:// gaukmotors.co.uk/, (Access Date: 12/01/2019).

[26] Web 7, (2019), https:// o4uxrk33.com/, (Access Date: 12/01/2019).

[27] Web 8, (2019), https://www.ansys.com/, (Access Date: 16/03/2019).

BIOGRAPHY

Duygu Basaran was born in Duzce, 1989. She received a Bachelor of Naval Architecture and Ocean Engineering in 2013 from Istanbul Technical University. In 2016, she started her master degree at Gebze Technical University, Natural and Applied Science department of mechanical engineering. During the following three years, she was employed as a design engineer in Norden Ship Design. Now, she is working as naval architect in Skipsteknisk.